Circulation

ORIGINAL RESEARCH ARTICLE

Selenoprotein P Promotes the Development of Pulmonary Arterial Hypertension

Possible Novel Therapeutic Target

Editorial, see p 624

Nobuhiro Kikuchi, MD, PhD
Kimio Satoh, MD, PhD
Ryo Kurosawa, MD
Nobuhiro Yaoita, MD, PhD
Md. Elias-Al-Mamun, PhD
Mohammad Abdul Hai Siddique, PhD
Junichi Omura, MD, PhD
Taijyu Satoh, MD, PhD
Masamichi Nogi, MD
Shinichiro Sunamura, MD
Satoshi Miyata, PhD
Yoshiro Saito, PhD
Yasushi Hoshikawa, MD, PhD
Yoshinori Okada, MD, PhD
Hiroaki Shimokawa, MD, PhD

BACKGROUND: Excessive proliferation and apoptosis resistance of pulmonary artery smooth muscle cells (PASMCs) are key mechanisms of pulmonary arterial hypertension (PAH). Despite the multiple combination therapy, a considerable number of patients develop severe pulmonary hypertension (PH) because of the lack of diagnostic biomarker and antiproliferative therapies for PASMCs.

METHODS: Microarray analyses were used to identify a novel therapeutic target for PAH. In vitro experiments, including lung and serum samples from patients with PAH, cultured PAH-PASMCs, and high-throughput screening of 3336 low-molecular-weight compounds, were used for mechanistic study and exploring a novel therapeutic agent. Five genetically modified mouse strains, including PASMC-specific selenoprotein P (SeP) knockout mice and PH model rats, were used to study the role of SeP and therapeutic capacity of the compounds for the development of PH in vivo.

RESULTS: Microarray analysis revealed a 32-fold increase in SeP in PAH-PASMCs compared with control PASMCs. SeP is a widely expressed extracellular protein maintaining cellular metabolism. Immunoreactivity of SeP was enhanced in the thickened media of pulmonary arteries in PAH. Serum SeP levels were also elevated in patients with PH compared with controls, and high serum SeP predicted poor outcome. SeP-knockout mice (*SeP*$^{-/-}$) exposed to chronic hypoxia showed significantly reduced right ventricular systolic pressure, right ventricular hypertrophy, and pulmonary artery remodeling compared with controls. In contrast, systemic SeP-overexpressing mice showed exacerbation of hypoxia-induced PH. Furthermore, PASMC-specific *SeP*$^{-/-}$ mice showed reduced hypoxia-induced PH compared with controls, whereas neither liver-specific SeP knockout nor liver-specific SeP-overexpressing mice showed significant differences with controls. Altogether, protein levels of SeP in the lungs were associated with the development of PH. Mechanistic experiments demonstrated that SeP promotes PASMC proliferation and resistance to apoptosis through increased oxidative stress and mitochondrial dysfunction, which were associated with activated hypoxia-inducible factor-1α and dysregulated glutathione metabolism. It is important to note that the high-throughput screening of 3336 compounds identified that sanguinarine, a plant alkaloid with antiproliferative effects, reduced SeP expression and proliferation in PASMCs and ameliorated PH in mice and rats.

CONCLUSIONS: These results indicate that SeP promotes the development of PH, suggesting that it is a novel biomarker and therapeutic target of the disorder.

Key Words: apoptosis ■ hypertension, pulmonary ■ hypoxia ■ mitochondria ■ oxidative stress

Sources of Funding, see page 621

https://www.ahajournals.org/journal/circ

Clinical Perspective

What Is New?

- Selenoprotein P (SeP) in pulmonary artery smooth muscle cells and serum from patients with pulmonary arterial hypertension (PAH) are elevated and promote cell proliferation and apoptosis resistance through increased oxidative stress and mitochondrial dysfunction, which are associated with activated hypoxia-inducible factor-1α and dysregulated glutathione metabolism.
- Using 5 strains of genetically modified mice, we demonstrated a pathogenic role of SeP in the development of hypoxia-induced pulmonary hypertension.
- Sanguinarine, an orally active small molecule identified by high-throughput screening, reduces SeP expression and pulmonary artery smooth muscle cell proliferation and ameliorates pulmonary hypertension.

What Are the Clinical Implications?

- SeP plays a crucial role in the pathogenesis of PAH and is also useful as a novel biomarker and therapeutic target of the disorder.
- Because conventional pulmonary vasodilators have limited efficacy for the treatment of severe PAH, sanguinarine with the antiproliferative effect on PAH–pulmonary artery smooth muscle cells can be a candidate for the novel therapeutic agent of the disease.
- The combination of SeP inhibitors and monitoring serum SeP levels, which may provide good candidates among patients with PAH, can be used to demonstrate the effectiveness of this strategy.

Pulmonary arterial hypertension (PAH) is characterized by histological changes in the distal pulmonary arteries, such as intimal lesions, medial thickening, and perivascular inflammation.[1] Pulmonary vascular remodeling and progressive obliteration of the vessel lumen increase vascular resistance and pulmonary arterial pressure, resulting in right ventricular (RV) failure and premature death.[2] In addition to genetic considerations, such as mutations in bone morphogenetic protein receptor 2,[3] many environmental factors, including hypoxia,[4] infection,[5] smoking,[6] air pollution,[7] sex hormones,[8,9] daily diet,[10] and medications,[11] as well as volume overload because of congenital heart disease[12] and inflammation because of collagen disease,[13] are involved in the development of PAH.[14] All of these factors constitute complex interactions that affect pulmonary vasculature in a multistage manner.[2,15] Thereby, vascular cells, especially pulmonary artery smooth muscle cells (PASMCs), will suffer epigenetic modifications, which recruit several transcriptional factors, such as hypoxia-inducible factor-1α (HIF-1α) and forkhead box protein O3a (FOXO3a),[16] to the promoter region of unknown pathogenic genes. Thus, the identification of these genes, which cause the abnormal characteristics of PASMCs, should be useful for the development of novel therapies for PAH.

The characteristics of PASMCs of patients with PAH (PAH-PASMCs) are different from those of healthy controls (control PASMCs) in terms of proproliferative and antiapoptotic features, which are similar to those of cancer cells.[17,18] However, we still have limited information as to the basal mechanism(s) of these characteristics. Recently, there has been active discussion on the abnormal features of PAH-PASMCs, particularly focusing on their mitochondrial dysfunction.[19] These features of PAH-PASMCs may be caused by some unknown pathogenic genes that promote PAH.[20] It is important to note that there seems to be a clue in the abnormal metabolism and continuous proliferation mechanism of cancer cells.[21] The Warburg effect is important for the maintenance of intracellular energy metabolism in cancer cells, suppressing mitochondrial ATP generation by glucose oxidation and increased glycolysis.[21] Here there are emerging theories of metabolic dysregulation in the pathogenesis of PAH, which is not restricted to PASMCs but also affects other extrapulmonary organs.[22–25] Thus, we assumed that the unknown pathogenic proteins in PAH-PASMCs could be secreted and detected in circulating blood, affect remote organs, and cause dysregulation of systemic metabolism.

To identify a novel pathogenic protein, we first performed microarray analyses using PAH-PASMCs and found 32-fold upregulation of selenoprotein P (SeP, encoded by *SEPP1*) compared with control PASMCs. SeP is a secreted protein mainly produced by hepatocytes, but it is also detected in many types of cells.[26,27] SeP contains 10 selenocysteine residues and transports selenium to maintain cellular redox state and metabolism.[28–31] Recently, it has been reported that SeP is upregulated in the liver of patients with type 2 diabetes mellitus and downregulates the metabolic switch, AMP-activated protein kinase (AMPK).[32] Moreover, single-nucleotide polymorphisms in the *SEPP1* gene have been reported to be associated with abdominal aortic aneurysm formation.[33] These findings suggest that SeP regulates cellular metabolism and the development of vascular diseases. Here, we report that SeP in PASMCs promotes cell proliferation through increased oxidative stress and mitochondrial dysfunction in an autocrine/paracrine manner. In addition, using 5 strains of genetically modified mice, we demonstrated a pathogenic role of SeP in the development of hypoxia-induced pulmonary hypertension (PH). Finally, we identified that sanguinarine, an orally active small molecule, reduces SeP expression and PASMC proliferation and ameliorates PH in mice and

rats. Thus, our data suggest that SeP could be a novel and realistic therapeutic target for PAH.

METHODS

Additional detailed methods are included in the online-only Data Supplement. The data that support the findings of this study are available from the corresponding author on reasonable request.

Human Lung Samples

All protocols using human specimens were approved by the Institutional Review Board of Tohoku University, Sendai, Japan (No. 2013-1-160). Lung tissues were obtained from patients with PAH at the time of lung transplantation (n=15) or from control patients (n=6) at the time of thoracic surgery for lung cancer at a site far from the tumor margins with normal lung parenchyma as previously described.[34,35] All patients provided written informed consent for the use of their lung tissues for the present study.

Isolation and Culture of Human Pulmonary Artery Endothelial Cells (PAECs) and PASMCs

PAH-PAECs were harvested from the lung tissue by elastase/collagenase digestion and isolated using CD31 antibody-coated magnetic beads.[36–38] Small pulmonary arteries were obtained from patients with PAH at the time of lung transplantation. PAH-PASMCs were isolated from pulmonary arteries <1.5 mm in outer diameter as previously described.[34,39] PASMCs were cultured in DMEM (Thermo Fisher Scientific) containing 10% fetal bovine serum (Thermo Fisher Scientific), and PAECs were cultured in endothelial cell basal medium-2 (Lonza) containing endothelial growth supplement (MV SingleQuots, Lonza) at 37°C in a humidified atmosphere of 5% CO_2 and 95% air. PAECs and PASMCs of passages 3 to 7 at 70% to 80% confluence were used for the experiments.

Microarray

Total RNA was extracted from PAH-PASMCs or control PASMCs cultured in DMEM containing 10% fetal bovine serum and penicillin-streptomycin (100 U/mL) (Thermo Fisher Scientific) and was quantified using NanoDrop 2000C (Thermo Fisher Scientific). Isolation of total RNA from PASMCs was performed using the RNeasy Plus Mini Kit (Qiagen) according to the manufacturer's instructions. For microarray expression profiling, samples were processed using the Agilent SurePrint G3 Human Gene Expression v3 8x60K Microarray Kit (Agilent Technologies) according to the manufacturer's instructions. The statistical computing software R (version 3.3.2.) and samr (version 2.0) package of R were used for preprocessing and statistical analysis. Differentially expressed genes were considered significant at significance analysis of microarrays *t* test *P* values of <0.05 and absolute values of logarithm of fold changes >1.0.[40] Genes with significant changes were further subjected to pathway analysis using ingenuity pathway analysis (http://www.ingenuity.com) to identify gene sets representing specific biological processes or functions.

Animal Experiments

All animal experiments were performed in accordance with the protocols approved by the Tohoku University Animal Care and Use Committee (No. 2015-Kodo-004) based on the ARRIVE trial (Animal Research: Reporting of In Vivo Experiments) guideline and the recent recommendations on optimal preclinical studies in PAH.[41] In all animal experiments, we used littermates or vehicle treatment groups as controls. The hypoxia-induced PH model of mice and Sugen/hypoxia-induced PH model of mice and rats were used to assess the development of PH.[34,35,42] In the hypoxia-induced PH model, 8-week-old male mice on a normal chow or Torula yeast-based diet that contained 1 mg of selenium/kg were exposed to hypoxia (10% O_2) or normoxia (21% O_2) for 3 or 4 weeks as previously described.[43–45] After 3 or 4 weeks of exposure to hypoxia or normoxia, mice were anesthetized with isoflurane (1.0%). To examine the development of PH, we measured hemodynamic parameters described later, RV hypertrophy (RVH), and pulmonary vascular remodeling.[34,35,43,44,46] For right heart catheterization, a 1.2-F (for mice) or 1.4-F (for rats) pressure catheter (Transonic Systems) was inserted into the right jugular vein and advanced into the RV to measure RV systolic pressure (RVSP) and RV end-diastolic pressure.[39] For left heart catheterization, the pressure catheter was inserted in the common carotid artery and advanced into the left ventricle (LV) to measure LV systolic pressure and LV end diastolic pressure. Cardiac output was measured using a thermodilution probe (AD Instruments). In the Sugen/hypoxia model, mice and rats (Sprague-Dawley, male, 7–10 weeks of age) were injected subcutaneously with the VEGF-receptor inhibitor SU5416 (Sigma-Aldrich) (20 mg/kg body weight) under isoflurane anesthesia and were then exposed to hypoxia (10% O_2) for 3 weeks according to previous reports.[42,46] After an indicated period of treatment, the animals were examined by treadmill exercise test, measuring hemodynamic parameters by echocardiography, and heart catheterization.

Seahorse Analysis

Oxygen consumption rate (OCR) and extracellular acidification rate (ECAR) were determined by the Seahorse XF 24-3 analyzer (Agilent). PASMCs or PAECs were plated onto cell culture microplates on the day before the experiments. On the day of the experiment, cells were exposed to normoxia (21% O_2) or hypoxia (1% O_2) for 4 hours. Control PAECs were pretreated with human SeP (10 μg/mL) or BSA (10 μg/mL) for 12 hours, followed by exposure to normoxia (21% O_2) or hypoxia (1% O_2) for 4 hours. Cells were incubated in XF assay medium (Agilent), supplemented with 25 mmol/L glucose and 1 mmol/L pyruvate (PASMCs) or 10 mmol/L glucose, 1 mmol/L pyruvate, and 2 mmol/L L-glutamine (PAECs) for 1 hour before the measurement. After the recording of the basal rates of OCR and ECAR, final concentrations of 1 μmol/L oligomycin, 1 μmol/L carbonyl cyanide-4 (trifluoromethoxy) phenylhydrazone, and 0.5 to 0.5 μmol/L rotenone and antimycin A for human PASMCs; 1 μmol/L oligomycin, 1 μmol/L carbonyl cyanide-4 (trifluoromethoxy) phenylhydrazone, and 1 to 1 μmol/L rotenone and antimycin A for human PAECs; and 2 μmol/L oligomycin, 0.5 μmol/L carbonyl cyanide-4 (trifluoromethoxy) phenylhydrazone, and 0.5 to 0.5 μmol/L rotenone and antimycin A for mouse PASMCs were added (XF Cell Mito Stress

Test Kit, Agilent) through the instrument's injection ports to obtain proton leak, maximal respiratory capacity, and nonmitochondrial respiration, respectively. Glycolytic capacity was measured using an XF Glycolysis Stress Test Kit (Seahorse Bioscience). Briefly, after incubation under normoxia or hypoxia, cells were washed in glucose-free XF assay medium (Agilent) containing 2 mmol/L L-glutamine at pH 7.35. ECAR was determined after serial injection with 10 mmol/L D-glucose, 1μmol/L oligomycin, and 100 mmol/L 2-deoxyglucose.

High-Throughput Screening

Libraries of drugs and bioactive compounds containing 3336 unique compounds were available from the Drug Discovery Initiative at the University of Tokyo (http://www.ddi.u-tokyo.ac.jp/en/). PAH-PASMCs were used for the first (proliferation assay) and second (reverse-transcriptional quantitative polymerase chain reaction) screening, and control PASMCs were used for counterassay (proliferation assay). PAH-PASMCs were trypsinized and resuspended in complete medium. They were counted, and 1000 cells/45 μL were plated in each well of a 384-well plate (catalog No. 781182, cell culture microplate 384 well, Greiner Bio-One) using the Multidrop Combi (Thermo Fisher Scientific). They were then placed in the automated incubator at 37°C for 24 hours. Fifteen μL of the diluted compounds were added to columns 3 to 22 of every plate by the Biomek NX^P (Beckman Coulter) (compounds 5 μmol/L, final concentration). The plates were incubated for an additional 48 hours, and the proliferation assay was performed using Cell Titer 96 AQueous One Solution Cell Proliferation Assay kit (Promega) according to the manufacturer's instructions. Hits were determined as compounds that suppressed PAH-PASMCs proliferation by >20% compared with control. The intra- and interplate variability in a pilot screen using 12 × 384–well plates showed a coefficient of variance of 5.9% and 4.0%, respectively.

Sanguinarine Treatment in Rats With Sugen/Hypoxia-Induced PH

Rats (Sprague-Dawley, male, 7–10 weeks of age) were injected subcutaneously with the VEGF-receptor inhibitor SU5416 (Sigma-Aldrich) (20 mg/kg body weight) under isoflurane anesthesia and were then exposed to hypoxia (10% O_2) for 3 weeks (hypoxia+SU5416).[46] On day 21, the animals were randomized to receive sanguinarine (5 mg/kg body weight) or vehicle via gavage under normoxia (21% O_2) for 4 weeks. Rats injected with saline on day 1 and exposed to normoxia for 7 weeks were used as a control group. Body weight and food consumption did not significantly differ between the sanguinarine and control groups. On day 49, the animals were examined by treadmill exercise test, measuring hemodynamic parameters by echocardiography, and heart catheterization.[47]

Statistical Analyses

All results are shown as mean±SEM. Comparisons of means between 2 groups were performed by unpaired Student's *t* test or 1-way ANOVA with interaction terms, followed by Tukey's honestly significant difference for multiple comparisons. Comparisons of mean responses associated with the 2 main effects of the different genotypes and the severity of pulmonary vascular remodeling were performed by 2-way ANOVA with interaction terms, followed by Tukey's honestly significant difference for multiple comparisons. To identify the cutoff point of the serum level of SeP that is able to classify patients with PH for all-cause death and lung transplantation, we performed the classification and regression trees analysis.[48] Statistical significance was evaluated with GraphPad Prism 7.02 (GraphPad Software, Inc) or R version 3.3.2 (http://www.R-project.org/). The time-dependent data were analyzed by repeated-measures linear mixed-effect model with lmer 1.1 to 12 and lmerTest 2.0 to 33 packages of R. The ratio of fully muscularized vessels was analyzed by the Poisson regression with the offset equals to the sum of total vessels with multcomp 1.4 to 6 package or R. All reported *P* values are 2-tailed, with a *P* value <0.05 indicating statistical significance.[34,35,46]

RESULTS

Screening of a Novel Therapeutic Target for PAH

To evaluate the altered phenotype of PAH-PASMCs, we established cell libraries of primary cultured PASMCs from patients with PAH undergoing lung transplantation (Figure 1A). To identify a novel therapeutic target for PAH, we performed a gene expression microarray screening using PAH-PASMCs and control PASMCs. The microarray analysis showed significant changes in 1858 genes, which were upregulated or downregulated in PAH-PASMCs compared with control PASMCs (Figure 1B). To select a target among the highly upregulated genes in PAH-PASMCs, we used the following selection criteria: (1) increase in the lungs of patients with PAH, (2) hypoxia-induced upregulation, and (3) circulating proteins in the blood (Figure 1B and Table I in the online-only Data Supplement). After rigorous analysis, we finally focused on SeP, which reproducibly showed a significant increase in PAH-PASMCs compared with control PASMCs (Figure 1C). Indeed, reverse-transcriptional quantitative polymerase chain reaction showed that PAH-PASMCs expressed 32-fold higher *SEPP1* compared with control PASMCs (Figure 1D). Because hypoxia is an important trigger for the development of PAH,[2] we regarded as highly important the hypoxia-induced increase in *SEPP1* in PAH-PASMCs (Figure 1E). To further confirm the protein levels of SeP in distal pulmonary arteries, we used lung tissues from patients with PAH. Western blot showed that the amount of SeP was significantly increased in the lungs from patients with PAH compared with those from controls (Figure 1F). Immunostaining showed that SeP was highly expressed in the thickened medial layer of distal pulmonary arteries in patients with PAH (Figure 1G). Consistently, protein levels of SeP were significantly increased in PAH-PASMCs compared with control PASMCs (Figure 1H). Moreover,

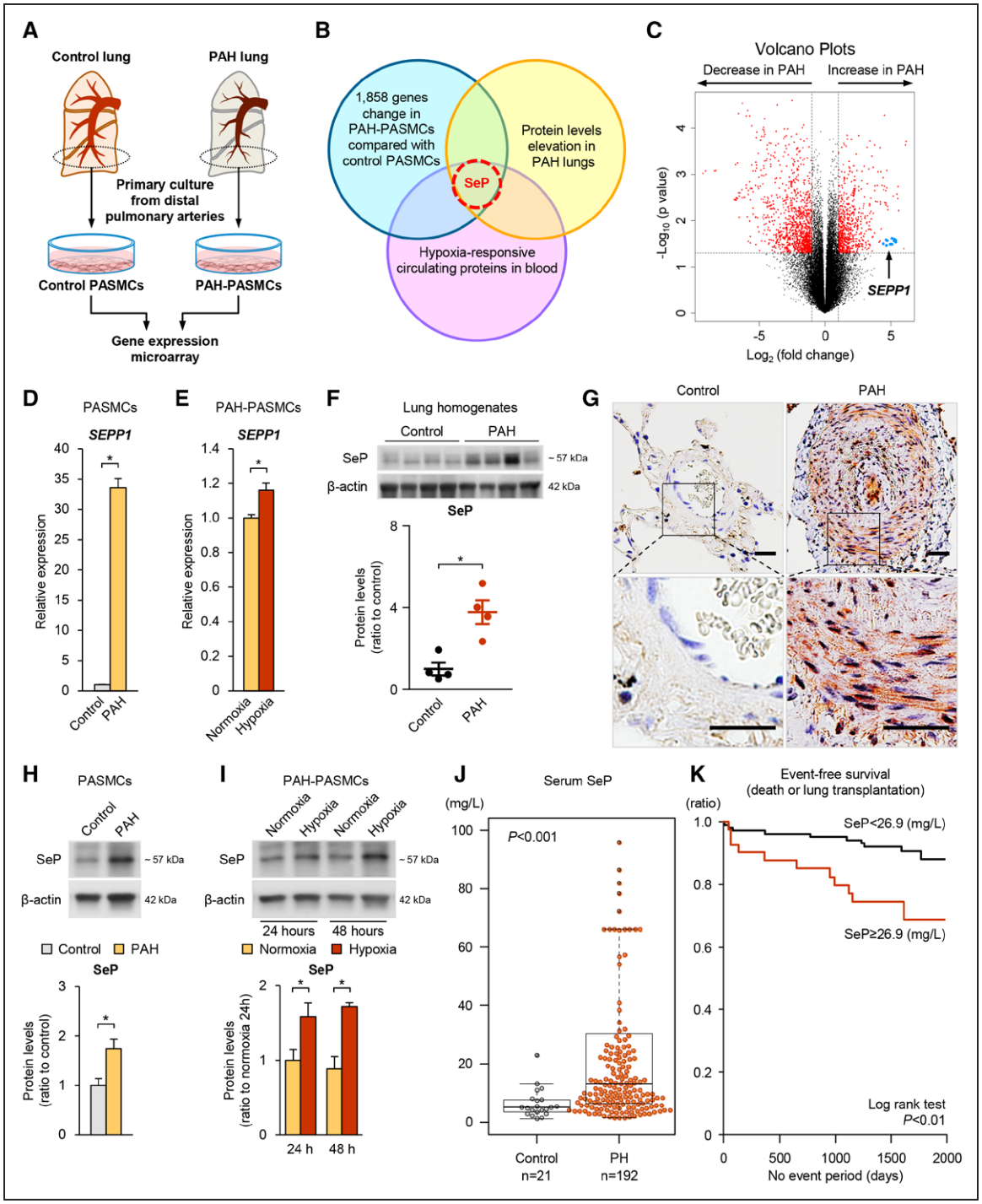

Figure 1. Screening of a novel therapeutic target for PAH.

A, Primary culture of pulmonary artery smooth muscle cells (PASMCs) from patients with pulmonary arterial hypertension (PAH). **B**, Schematic outline of screening to identify a novel therapeutic target of PAH. **C**, Volcano plots of gene expression variations in PAH-PASMCs and control PASMCs (n=4 each). Blue plots represent probes for *SEPP1*. Dashed lines represent an adjusted *P* value of 0.05 and ±1-fold change. **D**, Relative mRNA expression of *SEPP1* in PASMCs normalized to a *GAPDH* internal control (n=4 each). Values are expressed relative to control PASMCs. **E**, Relative mRNA expression of *SEPP1* in PAH-PASMCs in response to hypoxia (1% O_2) for 1 hour (n=6 each). Average expression values are normalized to a *GAPDH* internal control. Values are expressed relative to normoxia. **F**, Representative Western blots and quantification of selenoprotein P (SeP) and β-actin in the lungs of control patients and those with PAH (n=4 each). **G**, Representative immunostainings of the distal pulmonary arteries in patients with PAH who underwent lung transplantation. Scale bars, 20 μm. **H**, Representative Western blots and quantification of SeP levels in PAH-PASMCs and control PASMCs normalized to a β-actin internal control (n=4 each). Values are expressed relative to control PASMCs. **I**, Representative Western blots and quantification of SeP levels in PAH-PASMCs under normoxia (21% O_2) or hypoxia (1% O_2) for the indicated duration normalized to a β-actin internal control (n=6 each). Values are expressed relative to 24-hour normoxia. Data represent the mean±SEM. **P*<0.05. Comparisons of parameters were performed with the unpaired Student's *t* test or 2-way ANOVA, followed by Tukey's honestly significant difference test for multiple comparisons. **J**, Serum levels of SeP in patients with pulmonary hypertension (PH, n=192) and controls (n=21). Baseline characteristics of samples can be found in Table II in the online-only Data Supplement. Box-and-whisker and dot plots of serum levels of SeP. **K**, Kaplan-Meier curve of the 2 groups of PH patients according to the serum SeP levels (cutoff level, 26.9 mg/L). Baseline characteristics of samples can be found in Table III in the online-only Data Supplement. The outcome was death from any cause or lung transplantation. *P*<0.01, log rank test.

PAH-PASMCs showed further increase in SeP protein by hypoxic exposure compared with normoxic controls (Figure 1I). In contrast, hypoxia increased SeP protein levels in control PASMCs as well, and the increase was smaller than those in PAH-PASMCs (Figure I in the online-only Data Supplement). Because SeP is a secreted protein, we further performed ELISA to evaluate the serum levels of SeP in patients with PAH. It is important to note that serum SeP levels were significantly increased in patients with PAH compared with controls (Figure 1J), and the event-free survival curve showed that higher serum SeP levels predicted a poor outcome of patients with PAH (Figure 1K). These results support the notion that production of SeP in PASMCs and its release into the circulation are enhanced in patients with PAH compared with controls, which is further supported by the enhanced SeP expression in the lungs of those patients (Figure 1F and G). Here we compared the protein levels of SeP in PAH-PASMCs and the severity of PAH assessed by pulmonary vascular resistance in each patient. It is interesting to note that the SeP protein levels in PAH-PASMCs had a positive correlation with pulmonary vascular resistance in each patient with PAH (Figure II in the online-only Data Supplement). These results suggest that SeP in PASMCs is a potential pathogenic protein for the development of PAH. Consistent with the higher serum levels of SeP, serum selenium contents were significantly increased in patients with PAH compared with controls (Figure III in the online-only Data Supplement).

Selenoprotein P Deficiency Ameliorates Hypoxia-Induced PH In Vivo

We then examined a time-dependent increase in SeP protein in the lung in response to chronic hypoxia (10% O_2) in wild-type mice (Figure 2A). Thus, we used SeP-knockout (*Sepp1*$^{-/-}$) mice and littermate controls (*Sepp1*$^{+/+}$ mice) to evaluate the role of SeP in hypoxia-induced PH. *Sepp1*$^{-/-}$ mice showed no abnormal phenotypes under physiological conditions. The morphology of distal pulmonary arteries in normoxic *Sepp1*$^{-/-}$ mice did not differ from that of control mice (Figure 2B). In contrast, when exposed to hypoxia for 4 weeks, they exhibited a significant difference in the medial thickness of pulmonary arteries (Figure 2B). Compared with *Sepp1*$^{+/+}$ mice, *Sepp1*$^{-/-}$ mice showed fewer muscularized distal pulmonary arteries after hypoxic exposure (Figure 2C). Muscularized distal pulmonary arteries exhibited immunoreactivity for α–smooth muscle actin (Figure 2B). Consistent with these morphological changes, *Sepp1*$^{+/+}$ mice showed increased RVSP, which was attenuated in *Sepp1*$^{-/-}$ mice (Figure 2D). The increased ratio of RV to LV plus septum weight (RVH) was also attenuated in *Sepp1*$^{-/-}$ mice (Figure 2E), suggesting a crucial role for SeP in hypoxia-induced PH. It is interesting to note that SeP heterozygous knockout (*Sepp1*$^{+/-}$) mice also exhibited significantly less muscularization of distal pulmonary arteries and attenuated RVSP and RVH compared with *Sepp1*$^{+/+}$ mice, the extent of which was similar with those of *Sepp1*$^{-/-}$ mice (Figure IV in the online-only Data Supplement). These results indicate that 1 allele deletion of SeP is sufficient for prevention of the development of hypoxia-induced PH in mice.

To evaluate the role of SeP in cell proliferation, we harvested PASMCs from *Sepp1*$^{+/+}$ and *Sepp1*$^{-/-}$ mice. It is interesting to note that *Sepp1*$^{-/-}$ PASMCs showed reduced proliferation compared with *Sepp1*$^{+/+}$ PASMCs, in response to platelet-derived growth factor–BB (Figure 2F). Moreover, human SeP (hSeP) treatment promoted proliferation of PASMCs from both genotypes, which was significantly reduced in *Sepp1*$^{-/-}$ PASMCs compared with *Sepp1*$^{+/+}$ PASMCs (Figure 2G). The combination of platelet-derived growth factor–BB and hSeP further increased *Sepp1*$^{+/+}$ PASMC proliferation compared with platelet-derived growth factor–BB alone (Figure 2H). Consistently, Western blot analysis showed that *Sepp1*$^{-/-}$ PASMCs, compared with *Sepp1*$^{+/+}$ PASMCs, had reduced phosphorylation of extracellular signal-regulated kinase 1/2 (ERK1/2), Akt, and the mammalian target of rapamycin (Figure 2I). Thus, these results suggest that both intra- and extracellular SeP promote PASMC proliferation. Indeed, Western blot analysis of lung homogenates showed that Akt phosphorylation was significantly reduced in *Sepp1*$^{-/-}$ mice compared with *Sepp1*$^{+/+}$ mice (Figure 2J). In contrast, AMPK phosphorylation was significantly upregulated in the lungs of *Sepp1*$^{-/-}$ mice compared with *Sepp1*$^{+/+}$ mice (Figure 2J). Furthermore, *Sepp1*$^{-/-}$ mice showed reduced Ser253 phosphorylation and increased Ser294 phosphorylation of FOXO3a in the lung compared with *Sepp1*$^{+/+}$ mice (Figure 2J). FOXO3a is known to be a common target of ERK1/2, Akt, and AMPK, all of which regulate many genes involved in inflammation, cell proliferation, and metabolism.[49] Thus, we used the Bio-Plex multiplex system to evaluate the levels of cytokines/chemokines and growth factors in the lung and found a significant reduction in cytokines and chemokines (eg, interleukin-1β, chemokine [C-C motif] ligand 3, and macrophage colony-stimulating factor) in *Sepp1*$^{-/-}$ mice compared with *Sepp1*$^{+/+}$ mice after hypoxia (Figure VA in the online-only Data Supplement). Moreover, the secretion of these factors was also reduced in *Sepp1*$^{-/-}$ PASMCs compared with *Sepp1*$^{+/+}$ PASMCs (Figure VB in the online-only Data Supplement). These results suggest that SeP in PASMCs is important for inflammation and proliferation in an autocrine/paracrine manner.

Systemic Overexpression of SeP Promotes Hypoxia-Induced PH In Vivo

To evaluate the role of systemic SeP overexpression, we generated mice overexpressing SeP by using a SeP-encoding plasmid (CAG promoter-human *SEPP1*). The

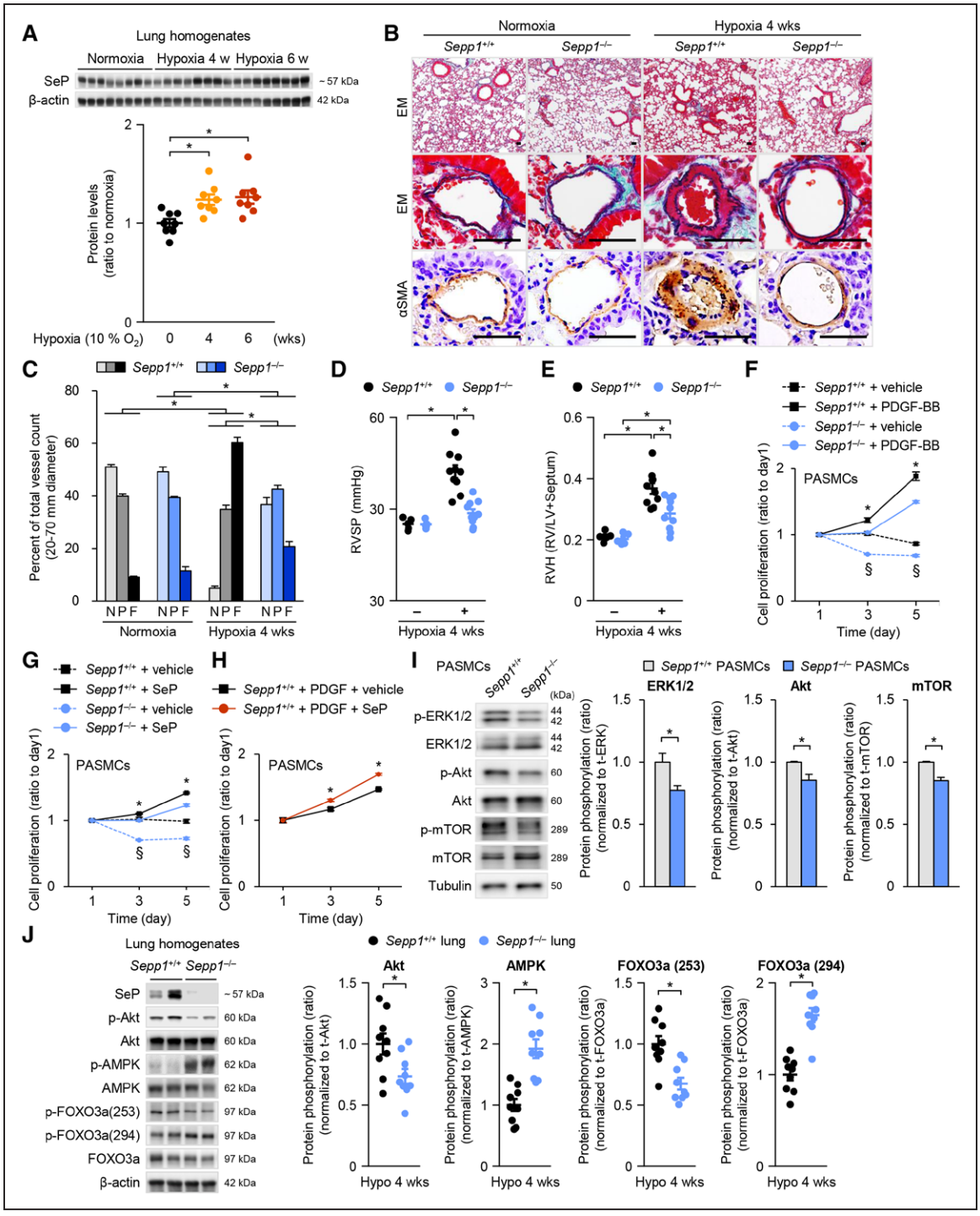

Figure 2. Selenoprotein P deficiency ameliorates hypoxia-induced PH in vivo.
A, Representative Western blots and quantification of selenoprotein P (SeP) protein levels in the lung under normoxia (21% O_2) or hypoxia (10% O_2) in wild-type mice (n=8 each). **B**, Representative Elastica-Masson (EM) and immunostainings for α–smooth muscle actin (αSMA) of the distal pulmonary arteries from *Sepp1*$^{+/+}$ and *Sepp1*$^{-/-}$ mice exposed to normoxia or hypoxia (10% O_2) for 4 weeks. Scale bars, 50 μm. **C**, Muscularization of the distal pulmonary arteries in *Sepp1*$^{+/+}$ and *Sepp1*$^{-/-}$ mice exposed to normoxia (n=5 each) or hypoxia (10% O_2) for 4 weeks (*Sepp1*$^{+/+}$, n=13; *Sepp1*$^{-/-}$, n=11). **D** and **E**, Right ventricular systolic pressure (RVSP) and right ventricular hypertrophy (RVH) in *Sepp1*$^{+/+}$ and *Sepp1*$^{-/-}$ mice exposed to normoxia (n=5 each) or hypoxia (10% O_2) for 4 weeks (n=10 each). **F**, Growth curve of *Sepp1*$^{+/+}$ and *Sepp1*$^{-/-}$ pulmonary artery smooth muscle cells (PASMCs) after treatment with or without platelet-derived growth factor–BB (PDGF-BB) (20 ng/mL) (n=8 each) after starvation for 24 hours. Values are expressed as a ratio relative to day 1. *P<0.05 compared with *Sepp1*$^{-/-}$ with PDGF-BB; §P<0.05 compared with *Sepp1*$^{+/+}$ with vehicle. **G**, Growth curve of *Sepp1*$^{+/+}$ and *Sepp1*$^{-/-}$ PASMCs after treatment with or without SeP (10 μg/mL) (n=8 each) after starvation for 24 hours. Values are expressed as a ratio relative to day 1. *P<0.05 compared with *Sepp1*$^{-/-}$ with SeP; §P<0.05 compared with *Sepp1*$^{+/+}$ with vehicle. **H**, Growth curve of *Sepp1*$^{+/+}$ PASMCs after PDGF-BB (20 ng/mL) treatment with or without SeP (10 μg/mL) after starvation for 24 hours (n=8 each). Values are expressed as a ratio relative to day 1. **I**, Representative Western blots and quantification of phospho-extracellular signal regulated kinases 1 and 2 (ERK1/2), phospho-Akt, and phospho-mechanistic target of rapamycin (mTOR) in *Sepp1*$^{+/+}$ and *Sepp1*$^{-/-}$ PASMCs without serum for 24 hours (n=6 each). **J**, Representative Western blots and quantification of phospho-Akt, (*Continued*)

systemic overexpressing mice (SeP-S) and mice with control plasmid (Ctrl-S) were then exposed to hypoxia for 3 weeks (Figure 3A). Western blot analysis showed that serum SeP levels were significantly higher in SeP-S mice compared with Ctrl-S mice (Figure 3B). Moreover, SeP in the lung was significantly increased in SeP-S mice compared with Ctrl-S mice (Figure 3C). It is important to note that SeP-S mice showed exacerbated remodeling of distal pulmonary arteries in response to hypoxia compared with Ctrl-S mice (Figure 3D). Consistent with these morphological changes, SeP-S mice showed significant increases in RVSP and RVH in response to hypoxia compared with Ctrl-S mice (Figure 3E). These results suggest that systemic overexpression of SeP promotes the development of hypoxia-induced PH.

Targeted Deletion of SeP in PASMCs Ameliorates Hypoxia-Induced PH

To evaluate the specific role of SeP in PASMCs, we developed a smooth muscle-specific SeP knockout mouse (*Sepp1*$^{flox/flox}$/*Sm22a-cre*$^{+/-}$; SMC-*Sepp1*$^{-/-}$) (Figure 4A). SMC-*Sepp1*$^{-/-}$ and control (*Sepp1*$^{flox/flox}$/*Sm22α-cre*$^{-/-}$) mice showed normal growth under physiological conditions. The morphology of pulmonary arteries in normoxic SMC-*Sepp1*$^{-/-}$ mice did not differ from that of control mice under normoxia (Figure 4B). In contrast, SMC-*Sepp1*$^{-/-}$ mice exhibited reduced muscularization of distal pulmonary arteries after hypoxic exposure compared with control mice (Figure 4B). It is important to note that SeP protein levels in the serum (Figure 4C) and the lungs (Figure 4D) were significantly lower in SMC-*Sepp1*$^{-/-}$ mice compared with control mice. Consistent with the morphological changes and SeP expression in the lung, SMC-*Sepp1*$^{-/-}$ mice showed reduced RVSP and RVH compared with control mice after 4 weeks of hypoxia (Figure 4E). These results suggest that SeP in PASMCs plays a crucial role in the development of hypoxia-induced PH.

SeP in the Liver Is Not Crucial for the Development of PH

Although we demonstrated a crucial role for SeP in PASMCs, 60% of SeP is synthesized in the liver and is released into the blood under physiological conditions.[26] Thus, to examine the role of liver-derived SeP in the development of PH, we used liver-specific SeP knockout (*Sepp1*$^{flox/flox}$/*Alb-cre*$^{+/-}$; Liver-*Sepp1*$^{-/-}$) mice (Figure VIA in the online-only Data Supplement). Liver-*Sepp1*$^{-/-}$ and control (*Sepp1*$^{flox/flox}$/*Alb-cre*$^{-/-}$) mice showed normal growth under physiological conditions and no significant difference in systolic blood pressure or laboratory data.[26] Serum levels of SeP were significantly lower in Liver-*Sepp1*$^{-/-}$ mice compared with control mice under both normoxia and hypoxia (Figure VIB in the online-only Data Supplement). After hypoxic exposure for 4 weeks, we found a 2.5-fold increase in serum SeP level in Liver-*Sepp1*$^{-/-}$ mice compared with a 1.4-fold increase in serum SeP level in controls (Figure VIB in the online-only Data Supplement). This finding suggests the crucial role of extrahepatic organs for a hypoxia-induced increase in serum levels of SeP. Hypoxia significantly and equally increased SeP levels (1.8-fold compared with normoxia) in the lungs of Liver-*Sepp1*$^{-/-}$ and control mice (Figure VIC in the online-only Data Supplement), suggesting the considerable contribution of the lungs in hypoxia-induced increase in serum levels of SeP. Moreover, the morphology of pulmonary arteries from Liver-*Sepp1*$^{-/-}$ and control mice did not differ under both normoxia and hypoxia (Figure VID in the online-only Data Supplement). Consistently, Liver-*Sepp1*$^{-/-}$ mice showed no difference in RVSP or RVH compared with control mice (Figure VIE in the online-only Data Supplement). These results suggest that hypoxia augments SeP production in the lungs and a resultant increase in serum levels, a consistent finding with the hypoxia-induced SeP production in PAH-PASMCs (Figure 1I).

Next, to further confirm the role of liver-derived SeP, we generated mice overexpressing SeP specifically in the liver by using an albumin promoter-driven recombinant plasmid (pLIVE-human *SEPP1*). The liver-specific SeP overexpressing mice (SeP-L) and mice with control plasmid (Ctrl-L) were then exposed to hypoxia for 3 weeks (Figure VIF in the online-only Data Supplement). Western blot analysis showed that serum levels of SeP were higher in SeP-L mice compared with Ctrl-L mice in both normoxia and hypoxia (Figure VIG in the online-only Data Supplement). In contrast, SeP in the lungs of SeP-L mice was comparable to that of Ctrl-L mice (Figure VIH in the online-only Data Supplement). Consistently, SeP-L mice showed no significant difference in RVSP or RVH compared with Ctrl-L mice (Figure VI-I in the online-only Data). Altogether, liver-specific genetically modified mice clearly demonstrated that liver-derived SeP is not crucial in the development of hypoxia-induced PH.

Both Intracellular and Extracellular SeP Promote PASMC Proliferation

Considering the importance of SeP in the development of PH in vivo, we performed mechanistic experiments

Figure 2 Continued. phospho-AMP-activated protein kinase (AMPK), phospho-forkhead box protein O3a (FoxO3a) (Ser253), and phospho-FOXO3a (Ser294) in *Sepp1*$^{+/+}$ and *Sepp1*$^{-/-}$ lung tissues after 4 weeks of hypoxia (10% O_2) (n=9 each). Data represent the mean±SEM. **P*<0.05. Comparisons of parameters were performed with the unpaired Student's *t* test or 2-way ANOVA, followed by Tukey's honestly significant difference test for multiple comparisons. F indicates fully muscularized vessels; Hypo, hypoxia; LV, left ventricle; N, nonmuscularized vessels; P, partially muscularized vessels; p-, phospho; RV, right ventricle; and w, weeks.

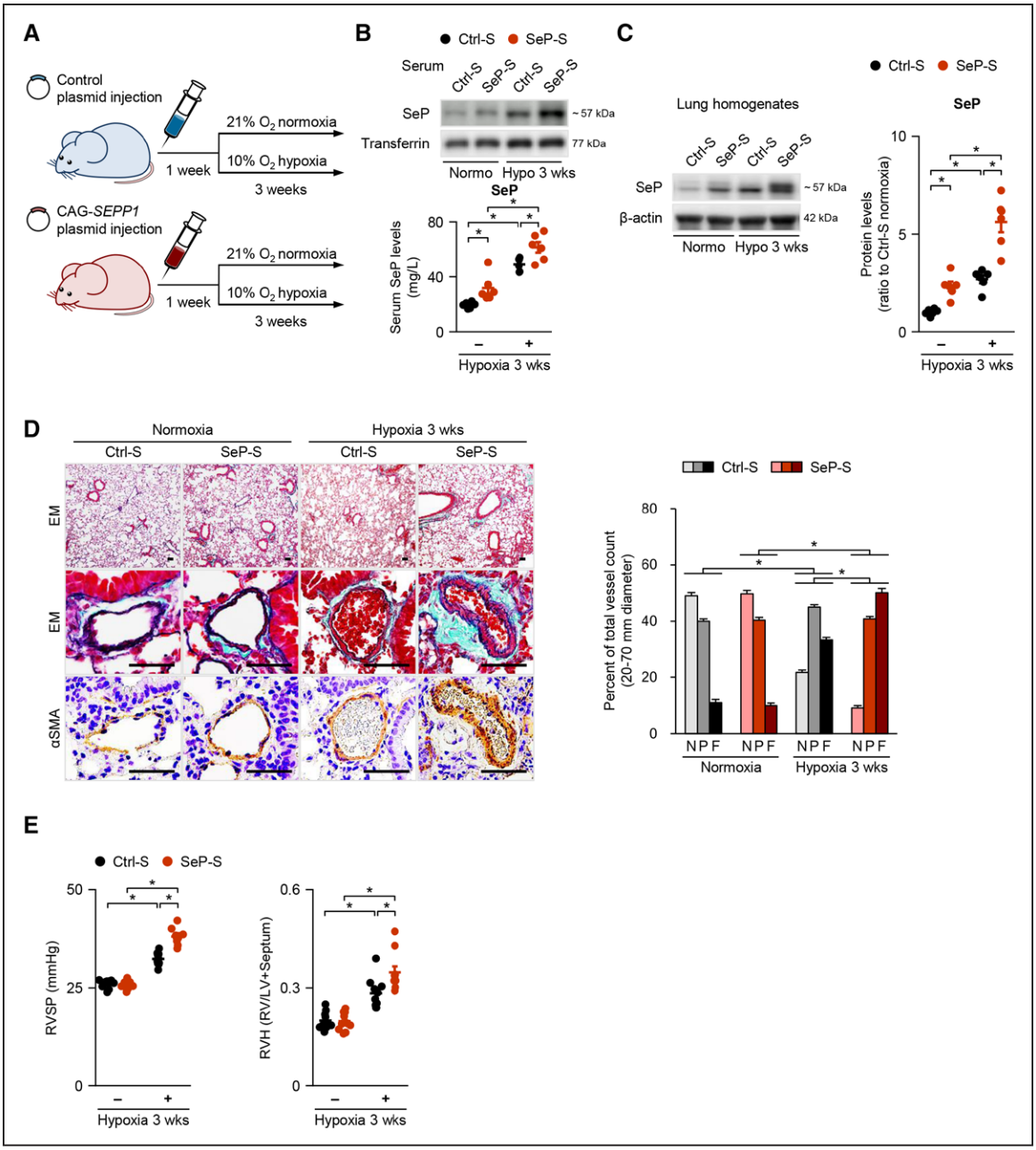

Figure 3. Systemic SeP overexpression in mice.
A, Schematic protocol of selenoprotein P (SeP) overexpression in wild-type mice. Human *SEPP1* plasmid DNA (SeP-P) or control plasmid DNA (Ctrl-P) were injected into the tail vein of wild-type mice. One week after injection, mice were exposed to normoxia or hypoxia (10% O_2) for 3 weeks. **B**, Representative Western blots and quantification of serum levels of SeP in SeP-P and Ctrl-P mice exposed to normoxia or hypoxia (10% O_2) for 3 weeks (n=6 each). **C**, Representative Western blots and quantification of SeP levels in the lungs of SeP-P and Ctrl-P mice exposed to normoxia or hypoxia (10% O_2) for 3 weeks (n=6 each). **D**, Left, representative Elastica-Masson (EM) and immunostaining for α-smooth muscle actin (αSMA) of the distal pulmonary arteries in SeP-P and Ctrl-P mice exposed to normoxia or hypoxia (10% O_2) for 3 weeks. Scale bars, 50 μm. Right, muscularization of the distal pulmonary arteries in SeP-P and Ctrl-P mice exposed to normoxia (Ctrl-P, n=10; SeP-P, n=11) or hypoxia (10% O_2) (n=10 each) for 3 weeks. **E**, Right ventricular systolic pressure (RVSP) (**left**) and right ventricular hypertrophy (RVH) (**right**) in SeP-P and Ctrl-P mice exposed to normoxia (Ctrl-P, n=10; SeP-P, n=11) or hypoxia (n=10 each) (10% O_2) for 3 weeks. Data represent the mean±SEM. *P<0.05. Comparisons of parameters were performed with 2-way ANOVA, followed by Tukey's honestly significant difference test for multiple comparisons. αSMA indicates α–smooth muscle actin; F, fully muscularized vessels; Hypo, hypoxia; LV, left ventricle; N, nonmuscularized vessels; Normo, normoxia; P, partially muscularized vessels; and RV, right ventricle.

using PAH-PASMCs and hSeP purified from human serum. Treatment of PAH-PASMCs with hSeP promoted cell proliferation compared with controls (Figure 5A). Consistently, hSeP treatment increased phosphorylation of ERK1/2 and Akt compared with controls (Figure 5B). Moreover, we detected increased Ser253 phosphorylation and reduced Ser294 phosphorylation of FOXO3a after hSeP treatment (Figure 5B). Consistently, reverse-transcriptional quantitative polymerase chain reaction analysis revealed increased expression of *CCND1*,

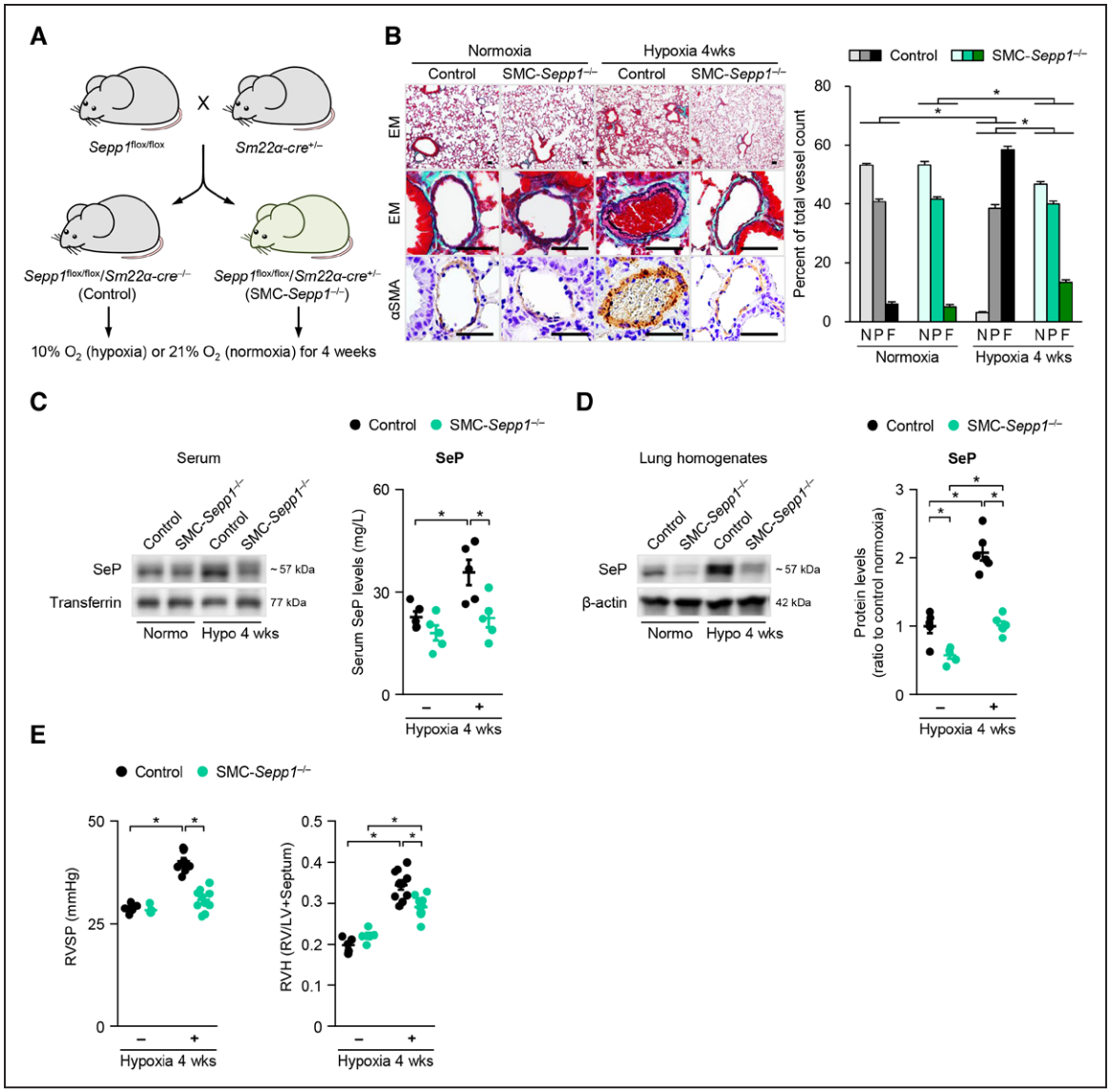

Figure 4. PASMC-specific deletion of selenoprotein P (SeP) ameliorates hypoxia-induced PH.
A, Schematic outline for generating smooth muscle cell (SMC)–specific SeP knockout mice. *Sepp1*$^{flox/flox}$, mice homozygous for the *Sepp1* conditional allele; *Sm22α-cre*$^{+/-}$, transgenic mice with Cre recombinase under the control of the *Sm22α* promoter. **B**, **Left**, representative Elastica-Masson (EM) and immunostainings for α–smooth muscle actin (αSMA) in distal pulmonary arteries of SMC-*Sepp1*$^{-/-}$ and control mice exposed to normoxia or hypoxia (10% O_2) for 4 weeks. Scale bars, 50 μm. **Right**, Muscularization of the distal pulmonary arteries in SMC-*Sepp1*$^{-/-}$ and control mice exposed to normoxia (n=5 each) or hypoxia (10% O_2) (control, n=13; SMC-*Sepp1*$^{-/-}$, n=10) for 4 weeks. **C** and **D**, Representative Western blots and quantification of SeP protein levels in the serum and the lungs of SMC-*Sepp1*$^{-/-}$ and control mice exposed to normoxia or hypoxia (10% O_2) for 4 weeks (n=5–6 each). **E**, Right ventricular (RV) systolic pressure (RVSP, **left**) and RV hypertrophy (RVH, **right**) in SMC-*Sepp1*$^{-/-}$ and control mice exposed to normoxia (n=5 each) or hypoxia (10% O_2) for 4 weeks (n=10 each). Data represent the mean±SEM. *P<0.05. Comparisons of parameters were performed with 2-way ANOVA, followed by Tukey's honestly significant difference test for multiple comparisons. F indicates fully muscularized vessels; Hypo, hypoxia; LV, left ventricle; N, nonmuscularized vessels; Normo, normoxia; P, partially muscularized vessels; PASMC, pulmonary artery smooth muscle cell; and PH, pulmonary hypertension.

a cell-cycle promoter, in response to hSeP treatment (Figure 5C). Moreover, hSeP treatment enhanced the expression of SeP (*SEPP1*) in PAH-PASMCs (Figure 5D), suggesting an autocrine/paracrine mechanism for the regulation of SeP expression. In addition to cell proliferation, SeP increased resistance to apoptosis in PAH-PASMCs under serum starvation (Figure VII in the online-only Data Supplement). In contrast, hSeP-mediated activation of intracellular signaling and mRNA changes were not found in control PASMCs (Figure VIII in the online-only Data Supplement), suggesting the importance of altered epigenetic backgrounds in PAH-PASMCs for SeP-mediated proliferation.

In addition to the role of extracellular SeP, we performed further analyses on the role of intracellular SeP in PAH-PASMCs. Knockdown of SeP by small interfering RNA (siRNA) markedly suppressed cell proliferation and apoptosis resistance in PAH-PASMCs compared with control siRNA (Figure 5E and Figure IX in the online-only Data Supplement). Consistently, SeP siRNA inacti-

vated ERK1/2 and Akt (Figure 5F) and increased Ser294 phosphorylation of FOXO3a (Figure 5G). Moreover, SeP siRNA increased the expression of *BCL2L11* (Bim) and *APLN* (Apelin) (Figure 5H), both of which block PASMC proliferation.[2] Recently, mounting evidence has indicated that dysfunctional DNA-damage response mechanisms promote resistance to apoptosis and antiproliferative phenotype of PAH-PASMCs.[50] Moreover, PAH-PASMCs have an upregulated critical enzyme implicated in DNA repair, poly (ADP-ribose) polymerase 1 levels, and subsequent downregulation of miR-204, which result in overexpression of bromodomain protein 4, HIF-1α, and NFAT, and finally promote their apoptosis-resistance.[51–53] We found that SeP inhibition by siRNA significantly reduced poly (ADP-ribose) polymerase 1 and bromodomain protein 4 levels in PAH-PASMCs (Figure XA in the online-only Data Supplement). In accordance with the reduced DNA repair, DNA damage was significantly increased by SeP knockdown assessed by DNA damage marker γ-histone H2AX (Figure XB in the online-only Data Supplement).

To further evaluate the role of intracellular SeP in PASMCs, we overexpressed SeP in control PASMCs using an SeP-encoding plasmid. Constitutive production of SeP in PASMCs (SeP-P) induced a 5-fold increase in SeP compared with the control plasmid (Ctrl-P), which increased cell proliferation in control PASMCs (Figure 5I). Consistently, SeP overexpression activated ERK1/2 and Akt and inactivated FOXO3a in control PASMCs (Figure 5J). These results suggest that both intracellular and extracellular SeP promote PASMC proliferation.

Synergistic Roles of SeP and HIF-1α in PASMC Proliferation

Hypoxia stabilizes HIF-1α, which promotes transcription of many genes that allow cells to adapt to hypoxic environment, especially in excessively proliferating cells.[21] It is interesting to note that Western blot analysis revealed increased HIF-1α in PAH-PASMCs compared with control PASMCs under both normoxic and hypoxic conditions (Figure 6A). Moreover, hSeP treatment further increased HIF-1α expression in PAH-PASMCs compared with controls (Figure 6B). In contrast, knockdown of SeP by siRNA significantly reduced HIF-1α expression in PAH-PASMCs compared with control siRNA (Figure 6C). Additionally, *Sepp1*$^{-/-}$ PASMCs showed significantly lower protein levels of HIF-1α compared with *Sepp1*$^{+/+}$ PASMCs under both normoxic and hypoxic conditions (Figure 6D). Conversely, knockdown of HIF-1α significantly reduced SeP expression in PAH-PASMCs compared with controls (Figure 6E), suggesting a synergistic interaction between SeP and HIF-1α expression in PAH-PASMCs. Next, we analyzed apolipoprotein E receptor 2 (ApoER2), 1 of the receptors for SeP.[28–31] It is important to note that PAH-PASMCs showed increased levels of AoER2 in mRNA and protein compared with control PASMCs (Figure 6F), which may explain in part the mechanisms for the augmented responses to extracellular hSeP. Moreover, ApoER2 siRNA significantly downregulated the expression of SeP and HIF-1α (Figure 6G). Consistently, ApoER2 siRNA significantly reduced hSeP-mediated proliferation of PAH-PASMCs (Figure 6H). In contrast, hSeP treatment increased ApoER2 expression in PAH-PASMCs (Figure 6I), suggesting a crucial role of ApoER2 in SeP-mediated proliferation of PASMCs. It is interesting to note that hSeP treatment increased heme oxygenase-1, which is induced in response to oxidative stress, in PAH-PASMCs (Figure 6J). Consistently, 2,7-dichlorodihydrofluorescein staining showed that hSeP treatment significantly increased oxidative stress levels in PAH-PASMCs (Figure 6K). Recent studies have shown that the pathogenesis of PAH is closely related with the increased oxidative stress, which is provoked by the lack of antioxidants, such as glutathione (GSH).[54,55] Here we found that the expression of glutathione synthase, glutamate-cysteine ligase catalytic subunit, and glutamate-cysteine ligase modulating subunit, all of which are responsible for GSH synthesis, were significantly reduced in PAH-PASMCs compared with those in control PASMCs under normoxia (Figure 6L). However, the expressions of glutamate-cysteine ligase catalytic and glutathione synthase in PAH-PASMCs were comparable to control PASMCs under hypoxic conditions. In contrast, the expression of glutamate-cysteine ligase modulating subunit was significantly lower in PAH-PASMCs compared with control PASMCs under hypoxia. Moreover, knockdown of HIF-1α significantly increased the expression of these enzymes in PAH-PASMCs (Figure 6M). Finally, we also found an hSeP-induced increase in ATP production in PAH-PASMCs (Figure 6N). These results suggest that SeP-mediated PASMC proliferation is induced by increased expression of ApoER2 and HIF-1α, reduced levels of GSH synthesis, and resultant increased oxidative stress levels in PAH-PASMCs (Figure 6O).

SeP-Mediated Mitochondrial Dysfunction in PAH-PASMCs

Considering the increased levels of SeP in PAH-PASMCs, we next focused on the role of SeP in the ability of intracellular metabolism to tolerate the hyperproliferative status. Indeed, recent studies of PAH showed an emerging role for metabolic abnormality in PAH-PASMCs.[19,20,22] Here, we detected higher levels of oxidative stress in PAH-PASMCs compared with control PASMCs under both normoxic and hypoxic conditions (Figure 7A and Figure XIA in the online-only Data Supplement). To evaluate the antioxidative capacity of PAH-PASMCs, we evaluated GSH levels by measuring reduced thiols. PAH-PASMCs showed significantly lower levels of GSH compared with control PASMCs under both normoxia and

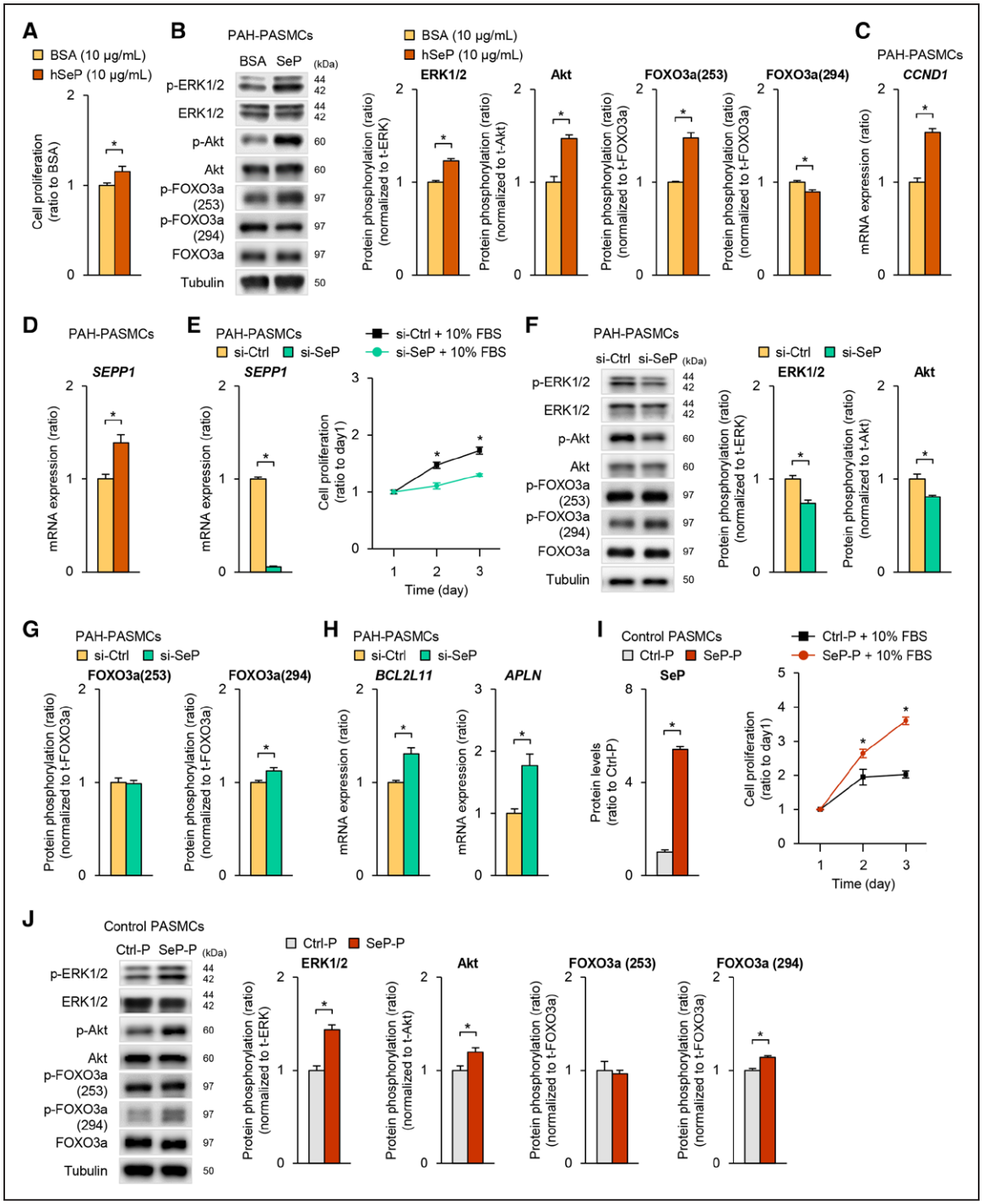

Figure 5. Selenoprotein P (SeP) promotes pulmonary artery smooth muscle cell (PASMC) proliferation.
A, Quantification of pulmonary arterial hypertension (PAH)–PASMC proliferation after starvation for 24 hours, followed by 48-hour treatment with human SeP (hSeP, 10 μg/mL) or bovine serum albumin (BSA, 10 μg/mL) (n=8 each). Values are expressed as a ratio relative to day 1. **B**, Representative Western blots and quantification of phospho-extracellular signal regulated kinases 1 and 2 (ERK1/2), phospho-Akt, phospho-forkhead box protein O3a (FoxO3a) (Ser253), and phospho-FOXO3a (Ser294) in PAH-PASMCs after treatment with hSeP or BSA (10 μg/mL each) for 24 hours (n=6 each). **C**, Reverse-transcriptional quantitative polymerase chain reaction (RT-PCR) analysis of *CCND1* mRNA in PAH-PASMCs after treatment with hSeP or BSA (10 μg/mL each) for 24 hours (n=6 each). Average expression values are normalized to *GAPDH* mRNA. **D**, RT-PCR analysis of *SEPP1* mRNA in PAH-PASMCs after treatment with hSeP or BSA (10 μg/mL each) for 24 hours (n=6 each). Average expression values are normalized to *GAPDH* mRNA. **E**, **Left**, RT-PCR analysis of *SEPP1* mRNA in PAH-PASMCs treated with control siRNA (si-Ctrl) or *SEPP1* siRNA (si-SeP) for 48 hours (n=6 each). Values are normalized to *GAPDH* mRNA. **Right**, Growth curve of PAH-PASMCs after treatment with si-Ctrl or si-SeP for 48 hours (n=8 each). Values are expressed as a ratio relative to day 1. **F**, Representative Western blots and quantification of phospho-ERK1/2 and phospho-Akt in PAH-PASMCs treated with si-Ctrl or si-SeP for 48 hours (n=6 each). **G**, Quantification of phospho-FOXO3a (Ser253) and phospho-FOXO3a (Ser294) in PAH-PASMCs treated with si-Ctrl or si-SeP for 48 hours (n=6 each). **H**, RT-PCR analysis of *BCL2L11* and *APLN* mRNA in PAH-PASMCs treated with si-Ctrl or si-SeP for 48 hours (n=6 each). Average expression values are normalized to *GAPDH* mRNA. **I**, **Left,** quantification of SeP protein levels in control PASMCs treated with human *SEPP1* plasmid DNA (SeP-P) or control plasmid (*Continued*)

hypoxia (Figure 7B). To elicit antioxidant effects, GSH is converted to oxidized glutathione (GSSG), and only free GSH has antioxidant effects.[56] GSSG lacks antioxidant functions and is a byproduct of the scavenging activity of GSH. Thus, the GSH/GSSG ratio is also important to assess the total capacity of reactive oxygen species (ROS) removal. We found significantly lower GSH levels and higher GSSG levels, which resulted in a lower GSH/GSSG ratio in PAH-PASMCs compared with control PASMCs under both normoxia and hypoxia (Figure 7C and Figure XIB in the online-only Data Supplement). These findings indicate the impaired capacity of PAH-PASMCs to remove ROS and resultant increased oxidative stress. Moreover, exogenously administered SeP increased oxidative stress levels and reduced antioxidative capacity in PAH-PASMCs (Figure XIC in the online-only Data Supplement). Additionally, we found that nicotinamide adenine dinucleotide phosphate (NADPH) oxidase activity was higher in PAH-PASMCs compared with control PASMCs (Figure XID in the online-only Data Supplement). Next, we examined the effects of SeP knockdown with siRNA. SeP siRNA canceled a hypoxia-mediated increase in ROS in PAH-PASMCs assessed by 2,7-dichlorodihydrofluorescein staining (Figure 7D). Consistently, SeP siRNA increased GSH levels in PAH-PASMCs, specifically in hypoxia (Figure 7E), supporting the importance of SeP for regulation of GSH levels in hypoxia. Conversely, to evaluate the significance of increased SeP in PAH-PASMCs, we overexpressed SeP in control PASMCs. SeP overexpression increased ROS levels compared with controls only in hypoxia (Figure 7F). Consistently, SeP overexpression attenuated a hypoxia-mediated increase in GSH levels in control PASMCs (Figure 7G), supporting the inhibitory role of SeP for hypoxia-mediated increase in GSH.[27] Here, selenium is a trace element that is contained in several antioxidant enzymes such as GPx and thioredoxin reductase.[57] Thus, to further confirm the involvement of selenium in the SeP-mediated inhibition of GSH, we prepared an SeP construct in which 10 selenocysteine residues are mutated to cysteine to delete selenium in SeP (Mut-P). Again, Mut-P overexpression increased ROS levels and reduced GSH in control PASMCs (Figure XIE in the online-only Data Supplement). These results suggest that SeP overexpression in control PASMCs reproduces a cell phenotype similar to PAH-PASMCs. To confirm the role of SeP as a modulator of ROS in PASMCs, we used *Sepp1*$^{+/+}$ and *Sepp1*$^{-/-}$ PASMCs. It is important to note that *Sepp1*$^{-/-}$ PASMCs showed significantly lower levels of ROS compared with *Sepp1*$^{+/+}$ PASMCs under both normoxia and hypoxia, which accompanied significant downregulation of NADPH oxidase activities in *Sepp1*$^{-/-}$ PASMCs compared with *Sepp1*$^{+/+}$ PASMCs (Figure 7H and Figure XIF and G in the online-only Data Supplement). Consistently, GSH levels were higher in *Sepp1*$^{-/-}$ PASMCs compared with *Sepp1*$^{+/+}$ PASMCs, especially in hypoxia (Figure 7I). Moreover, the GSH/GSSG ratio was significantly elevated in *Sepp1*$^{-/-}$ PASMCs compared with *Sepp1*$^{+/+}$ PASMCs under both normoxia and hypoxia (Figure 7J). These results suggest that higher SeP is 1 of the mechanistic explanations for the increased ROS in PAH-PASMCs. Using a Seahorse XF24-3 apparatus, which provides information on mitochondrial function through real-time measurements of OCR (a marker of oxidative phosphorylation) and ECAR (a surrogate for glycolysis), we examined hypoxia-induced responses in PAH-PASMCs and control PASMCs (Figure 7K). OCR reflects the mitochondrial respiration rate and energy production, and ECAR reflects the rate of glycolysis in PASMCs. Here we found significantly lower levels of the OCR/ECAR ratio and maximal OCR in PAH-PASMCs compared with control PASMCs (Figure 7L and Figure XIIA and B in the online-only Data Supplement). Moreover, hypoxic exposure further reduced OCR and the OCR/ECAR ratio compared with normoxia in both PAH-PASMCs and control PASMCs. In contrast, nonmitochondrial respiration and glycolysis were augmented in PAH-PASMCs compared with control PASMCs, demonstrating the shift of energy metabolism from oxidative phosphorylation to glycolysis (Figure XIIC in the online-only Data Supplement).[20] Indeed, dysregulated mitochondria in PAH-PASMCs show mitochondrial hyperpolarization, lower mitochondrial ROS (mROS) production, and inhibition of redox-sensitive Kv channels leading to vasoconstriction.[58–60] Consistently, PAH-PASMCs showed increased mitochondrial membrane potential ($\Delta\Psi$m) compared with control PASMCs under both normoxia and hypoxia (Figure XIID in the online-only Data Supplement). Moreover, exogenously administered SeP further increased $\Delta\Psi$m in PAH-PASMCs (Figure XIIE in the online-only Data Supplement). Additionally, mROS levels were lower in PAH-PASMCs compared with control PASMCs under both normoxia and hypoxia, which was further reduced by SeP treatment (Figure XIIF and G in the online-only Data Supplement). It is important to note that blocking the production of SeP by siRNA ameliorated the hypoxia-induced downregulation of mROS in PAH-PASMCs (Figure XIIH in the online-only Data Supplement. In contrast, SeP overexpression in control PASMCs reduced the levels of mROS, which were similar in PAH-PASMCs (Figure XII-I in the online-only Data

Figure 5 Continued. DNA (Ctrl-P) for 48 hours (n=6 each). **Right,** growth curve of control PASMCs after treatment with Ctrl-P or SeP-P for 48 hours (n=8 each). Values are expressed as a ratio relative to day 1. **J**, Representative Western blots and quantification of phospho-ERK1/2, phospho-Akt, phospho-FOXO3a (Ser253), and phospho-FOXO3a (Ser294) in control PASMCs treated with Ctrl-P or SeP-P for 48 hours (n=6 each). Data represent the mean±SEM. *P<0.05, unpaired Student's t test. FBS indicates fetal bovine serum p-, phospho; and si, small interfering.

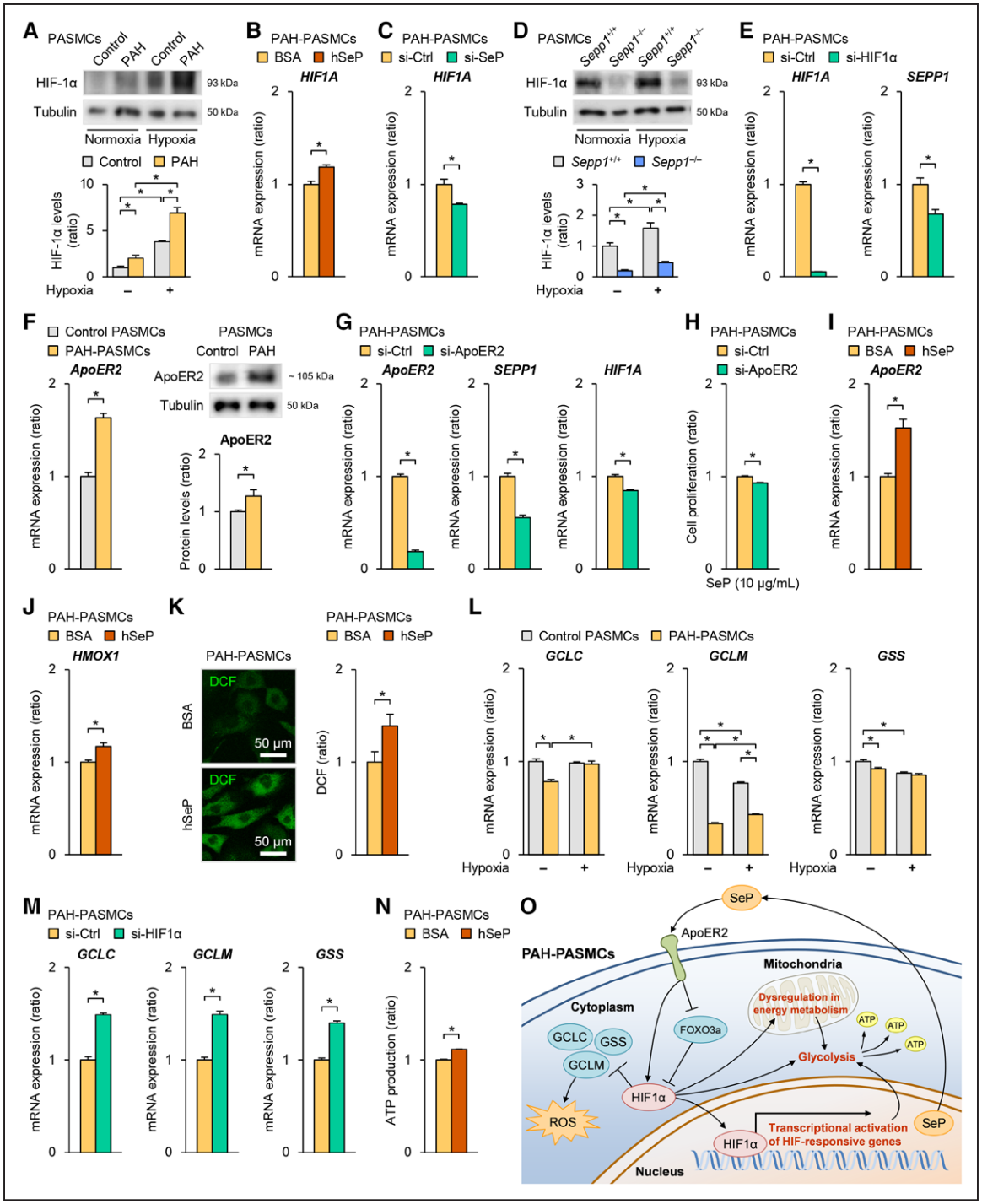

Figure 6. Synergistic roles of selenoprotein P (SeP) and hypoxia-inducible factor 1α (HIF-1α) in PASMC proliferation.
A, Representative Western blots and quantification of HIF-1α protein levels in pulmonary arterial hypertension (PAH)-pulmonary artery smooth muscle cells (PASMCs) and control PASMCs after exposure to normoxia (21% O_2) or hypoxia (1% O_2) for 2 hours (n=6 each). **B**, Reverse-transcriptional quantitative polymerase chain reaction (RT-PCR) analysis of *HIF1A* mRNA in PAH-PASMCs treated with human SeP (hSeP, 10 μg/mL) or bovine serum albumin (BSA, 10 μg/mL) for 24 hours (n=6 each). Average expression values are normalized to *GAPDH* mRNA. **C**, RT-PCR analysis of *HIF1A* mRNA in PAH-PASMCs treated with control siRNA (si-Ctrl) or *SEPP1* siRNA (si-SeP) for 48 hours (n=6 each). Average expression values are normalized to *GAPDH* mRNA. **D**, Representative Western blots and quantification of HIF-1α protein levels in *Sepp1*$^{+/+}$ and *Sepp1*$^{-/-}$ PASMCs after exposure to normoxia (21% O_2) or hypoxia (1% O_2) for 2 hours (n=6 each). **E**, RT-PCR analysis of *HIF1A* and *SEPP1* mRNA in PAH-PASMCs treated with si-Ctrl or *HIF1A* siRNA (si-HIF-1α) for 48 hours (n=6 each). Values are normalized to *GAPDH* mRNA. **F**, RT-PCR analysis of apolipoprotein E receptor 2 (*ApoER2*) mRNA and Western blot analysis of ApoER2 protein in PAH-PASMCs and control PASMCs (n=6 each). Average expression values are normalized to *GAPDH* mRNA. **G**, RT-PCR analysis of *ApoER2*, *SEPP1*, and *HIF1A* mRNA in PAH-PASMCs treated with si-Ctrl or *ApoER2* siRNA (si-ApoER2) for 48 hours (n=6 each). Values are normalized to *GAPDH* mRNA. **H**, Quantification of hSeP (10 μg/mL)–mediated proliferation in PAH-PASMCs after treatment with si-Ctrl or si-ApoER2 for 48 hours (n=8 each). Values are expressed as a ratio relative to control. **I**, RT-PCR analysis of *ApoER2* mRNA in PAH-PASMCs after treatment with hSeP or BSA (10 μg/mL each) for 24 hours (n=6 each). Average expression values are normalized to *GAPDH* mRNA. **J**, RT-PCR analysis of *HMOX1* mRNA in PAH-PASMCs after treatment with hSeP or BSA (10 μg/mL each) for 24 hours (n=6 each). Average expression values are normalized to *GAPDH* mRNA. **K**, **Left,** Representative images of 2,7-dichlorodihydrofluorescein (DCF) fluorescence in PAH-PASMCs after treatment (*Continued*)

Supplement). Recently, mounting evidence indicates that mitochondrial dynamics are relevant to the mechanisms of apoptosis, cell proliferation, and mitochondrial energy metabolism in PAH, like cancer cells.[61] PAH-PASMCs show increased dynamin-related protein–1 and reduced mitofusin-2, promoting impaired mitochondrial fusion, increased fission, and fragmentation of the mitochondrial networks in PASMCs.[62,63] Thus, we next examined the morphologies of mitochondria in control and PAH-PASMCs. Consistent with a recent report,[64] PAH-PASMCs showed more fragmented mitochondrial morphology compared with control PASMCs (Figure 7M). Next, we further examined hypoxia-mediated metabolic changes in *Sepp1*$^{+/+}$ and *Sepp1*$^{-/-}$ PASMCs (Figure 7N). We found a significantly higher OCR/ECAR ratio and maximal OCR in *Sepp1*$^{-/-}$ PASMCs compared with *Sepp1*$^{+/+}$ PASMCs (Figure 7O and Figure XIIIA and B in the online-only Data Supplement). Moreover, hypoxic exposure reduced the OCR/ECAR ratio and maximal OCR compared with normoxia in both *Sepp1*$^{+/+}$ and *Sepp1*$^{-/-}$ PASMCs. In contrast, glycolysis was lower in *Sepp1*$^{-/-}$ PASMCs compared with *Sepp1*$^{+/+}$ PASMCs, demonstrating the shift of energy metabolism from glycolysis to oxidative phosphorylation (Figure XIIIC in the online-only Data Supplement). Consistent with the upregulated mitochondrial function, *Sepp1*$^{-/-}$ PASMCs showed higher levels of mROS compared with *Sepp1*$^{+/+}$ PASMCs under both normoxia and hypoxia (Figure XIIID in the online-only Data Supplement). Moreover, *Sepp1*$^{-/-}$ PASMCs showed increased mitochondrial networks compared with *Sepp1*$^{+/+}$ PASMCs (Figure 7P). Consistent with the effects of SeP on mROS, mitochondrial membrane potential, and its metabolism, we found that SeP inhibition significantly reduced protein levels of survivin in PAH-PASMCs (Figure XIIIE in the online-only Data Supplement). Survivin mediates apoptosis resistance through mitochondrial membrane hyperpolarization in PAH-PASMCs.[53] We found that exogenously administered SeP caused phosphorylation of dynamin-related protein–1 at serine 616 (but not at serine 637) and increased the expression of pyruvate dehydrogenase kinase 1 in PAH-PASMCs (Figure XIIIF in the online-only Data Supplement). Mitochondrial fission is induced by phosphorylation of dynamin-related protein-1at Ser616 and inhibited by phosphorylation at Ser637.[64] Moreover, HIF-1α activates pyruvate dehydrogenase kinase, inhibits pyruvate dehydrogenase, and suppresses mitochondrial glucose oxidation.[22] Thus, SeP promotes mitochondrial fission and suppresses mitochondrial respiration. These results suggest that the balance between mitochondrial fission and fusion is fundamentally regulated by intracellular SeP levels in PASMCs. Additionally, SeP promotes switching from oxidative phosphorylation to anaerobic metabolism as an adaptive response to mitochondrial dysfunction, especially in hypoxia (Figure XIV in the online-only Data Supplement).

SeP-Mediated Dysregulation of PAECs

It has been clearly demonstrated that PAH-PAECs with loss of bone morphogenetic protein receptor 2 are susceptible to apoptosis as a result of a dysregulation in PPARγ/β-catenin/apelin signaling axis, resulting in a reduced number of peripheral PAs.[2] Thus, we next examined the role of SeP in PAECs. First, we compared the expression of SeP in PAH-PAECs and control PAECs and found that the SeP expression was significantly higher in PAH-PAECs compared with control PAECs under both normoxia and hypoxia (Figure XVA in the online-only Data Supplement). Second, we examined the mitochondrial function and glycolytic capacity in control PAECs and found upregulation of both OCR and ECAR by treatment with human SeP compared with BSA controls under both normoxia and hypoxia (Figure XVB in the online-only Data Supplement). Moreover, hypoxic exposure reduced OCR and increased ECAR in PAECs in BSA controls. In contrast, SeP treatment prevented the hypoxia-induced reduction in OCR and kept it at higher levels or even showed an increase in ECAR compared with BSA controls (Figure XVB in the online-only Data Supplement). Indeed, excessively enhanced mitochondrial oxidative phosphorylation has been shown to induce endothelial dysfunction and apoptosis, contributing to pulmonary vascular remodeling.[65,66] Thus, we next examined the PAEC viability by treatment with human SeP for 12 hours. Consistent with the results in OCR and ECAR, SeP treatment significantly reduced cell proliferation and induced apoptosis in PAECs after serum starvation (Figure XVC and D in the online-only Data Supplement).

Figure 6 Continued. with hSeP or BSA (10 μg/mL each) for 24 hours. Scale bars, 50 μm. **Right,** Quantification of DCF fluorescence intensity in PAH-PASMCs after treatment with hSeP or BSA (10 μg/mL each) for 24 hours (n=8 each). Values are normalized to cell numbers with BSA treatment. **L**, RT-PCR analysis of glutamate-cysteine ligase catalytic subunit (*GCLC*), glutamate-cysteine ligase modulating subunit (*GCLM*), and glutathione synthase (*GSS*) mRNA in PAH-PASMCs and control PASMCs after exposure to normoxia (21% O_2) or hypoxia (1% O_2) for 4 hours (n=6 each). Average expression values are normalized to *GAPDH* mRNA. **M**, RT-PCR analysis of *GCLC*, *GCLM*, and *GSS* mRNA in PAH-PASMCs treated with si-Ctrl or si-HIF-1α for 48 hours (n=6 each). Values are normalized to *GAPDH* mRNA. **N,** Quantitation of ATP production in PAH-PASMCs after treatment with hSeP or BSA (10 μg/mL each) for 1 hour (n=8 each). Values are normalized to cell numbers with BSA treatment. **O**, Schematic representation of the molecular mechanisms promoting SeP expression by HIF-1α activation and forkhead box protein O3a (FoxO3a) inactivation. Extracellular SeP induces oxidative stress, HIF-1α activation, and FOXO3a inactivation via SeP-ApoER2 signaling in PAH-PASMCs. Constitutively active HIF-1α induces transcription of many genes and dysregulation of mitochondrial energy metabolism, which promotes cell proliferation, apoptosis resistance, survival, and stress resistance by targeting several downstream genes, including SeP. ROS, reactive oxygen species. Throughout, data represent the mean±SEM. *P<0.05. Comparisons of parameters were performed with the unpaired Student's t test or 2-way ANOVA, followed by Tukey's honestly significant difference test for multiple comparisons. si indicates small interfering.

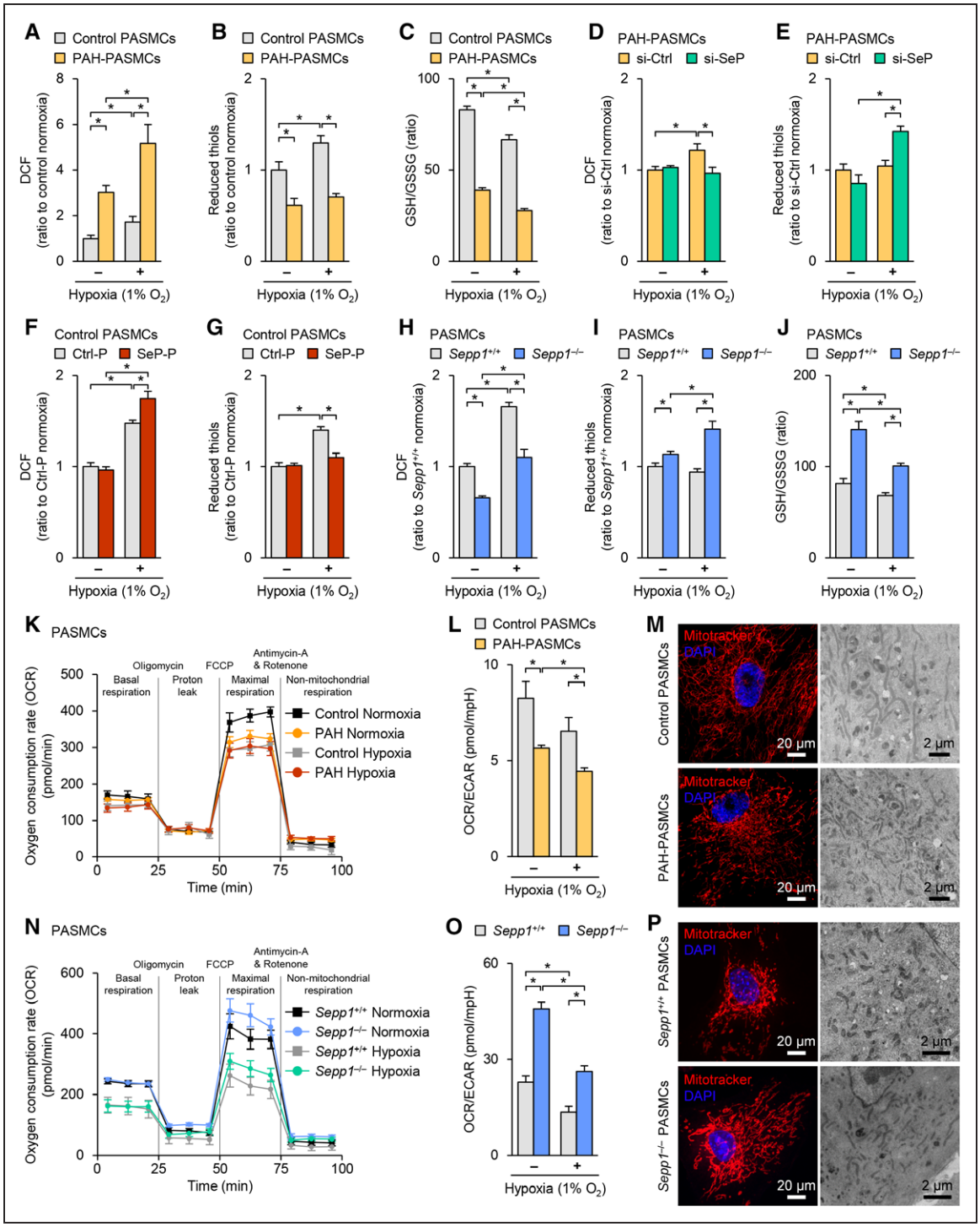

Figure 7. Selenoprotein P (SeP)–mediated mitochondrial dysfunction in pulmonary arterial hypertension (PAH)–pulmonary artery smooth muscle cells (PASMCs).

A, Quantification of 2,7-dichlorodihydrofluorescein (DCF) fluorescence intensity in PAH-PASMCs and control PASMCs after exposure to normoxia (21% O_2) or hypoxia (1% O_2) for 4 hours (n=8 each). **B**, Quantification of reduced thiols in PAH-PASMCs and control PASMCs after exposure to normoxia (21% O_2) or hypoxia (1% O_2) for 4 hours (n=8 each). **C**, Quantification of GSH/GSSG ratio in PAH-PASMCs and control PASMCs after exposure to normoxia (21% O_2) or hypoxia (1% O_2) for 4 hours (n=8 each). GSH, glutathione; GSSG, oxidized glutathione. **D**, Quantification of DCF fluorescence intensity in PAH-PASMCs after treatment with control siRNA (si-Ctrl) or *SEPP1* siRNA (si-SeP) for 48 hours, followed by exposure to normoxia (21% O_2) or hypoxia (1% O_2) for 4 hours (n=8 each). **E**, Quantification of reduced thiols in PAH-PASMCs treated with si-Ctrl or si-SeP for 48 hours, followed by exposure to normoxia (21% O_2) or hypoxia (1% O_2) for 4 hours (n=8 each). **F**, Quantification of DCF fluorescence intensity in human control PASMCs treated with human *SEPP1* plasmid DNA (SeP-P) or control plasmid DNA (Ctrl-P) for 48 hours, followed by exposure to normoxia (21% O_2) or hypoxia (1% O_2) for 4 hours (n=8 each). **G**, Quantification of reduced thiols in control PASMCs after treatment with Ctrl-P or SeP-P for 48 hours, followed by exposure to normoxia (21% O_2) or hypoxia (1% O_2) for 4 hours (n=8 each). **H**, Quantification of DCF fluorescence intensity in *Sepp1*$^{+/+}$ and *Sepp1*$^{-/-}$ PASMCs after exposure to normoxia (21% O_2) or hypoxia (1% O_2) for 4 hours (n=8 each). **I**, Quantification of reduced thiols in *Sepp1*$^{+/+}$ and *Sepp1*$^{-/-}$ PASMCs after exposure to normoxia (21% O_2) or hypoxia (1% O_2) for 4 hours (n=8 each). (*Continued*)

Sanguinarine Downregulates SeP and Ameliorates PH in Animal Models

Based on the experimental findings on the crucial role of SeP in PASMC proliferation, we then aimed to identify a therapeutic agent to downregulate SeP. For this purpose, we performed *in silico* screening with the Life Science Knowledge Bank software (http://www.lskb.w-fusionus.com/) and found that there is no compound with an inhibitory effect on SeP. Then we used the public chemical library in the Drug Discovery Initiative (http://www.ddi.u-tokyo.ac.jp/en/), a collection of 3336 clinically used compounds and derivatives. We performed a high-throughput screening and identified 3 compounds that reduce SeP expression and proliferation of PAH-PASMCs (Figure 8A). Among them, we focused on sanguinarine, a benzophenanthridine alkaloid derived from the root of *Sanguinaria Canadensis*, with antiproliferative effects against cancers.[67] We found that sanguinarine treatment reduced SeP expression and cell proliferation and induced apoptosis in PAH-PASMCs (Figure 8B and Figure XVI in the online-only Data Supplement). Consistently, we found that SeP inhibition by sanguinarine downregulated poly (ADP-ribose) polymerase 1 and bromodomain protein 4 compared with vehicle controls, resulting in a significant increase of DNA damage in PAH-PASMCs (Figure XVII in the online-only Data Supplement). Administration of sanguinarine upregulated mitochondrial respiration in PAH-PASMCs compared with vehicle controls (Figure XVIIIA in the online-only Data Supplement). Consistently, SeP inhibition by sanguinarine reduced survivin proteins in PAH-PASMCs (Figure XVIIIB in the online-only Data Supplement). We then examined the effect of oral administration of sanguinarine in hypoxia-induced PH in mice (Figure XVIIIC in the online-only Data Supplement). Daily administration of sanguinarine via gavage during 28 days of chronic hypoxia had no effect on body weight or food consumption compared with vehicle controls (Figure XVIIID in the online-only Data Supplement). A hypoxia-induced increase in SeP in the lungs was significantly attenuated by sanguinarine treatment compared with vehicle controls (Figure 8C). In contrast, protein levels of SeP in the liver did not change in response to sanguinarine treatment (Figure XVIIIE in the online-only Data Supplement). Moreover, sanguinarine significantly reduced the serum levels of SeP especially after hypoxic exposure (Figure 8D). Sanguinarine significantly suppressed muscularization of distal pulmonary arteries after hypoxic exposure compared with vehicle controls (Figure 8E). Consistently, sanguinarine significantly ameliorated hypoxia-induced increases in RVSP and RVH compared with vehicle controls (Figure 8F). Next, to further evaluate the therapeutic potential of sanguinarine for PAH, we used another animal model of PH, in which rats were exposed to chronic hypoxia for 21 days in combination with an injection of SU5416 (Sugen/hypoxia model) (Figure XVIIIF in the online-only Data Supplement). In this Sugen/hypoxia rat model, we started sanguinarine treatment after development of PH (treatment protocol). Daily administration of sanguinarine via gavage for 28 days had no effect on body weight or food consumption compared with vehicle controls (Figure XVIIIG in the online-only Data Supplement). Protein levels of SeP in the lungs were significantly elevated in the Sugen/hypoxia rat model (Figure 8G), and were significantly reduced by sanguinarine treatment. Consistently, sanguinarine treatment significantly reduced RVSP, RV end diastolic pressure, and RVH and increased cardiac output compared with vehicle controls (Figure 8H and I and Figure XIXA in the online-only Data Supplement). Sanguinarine also improved hemodynamic parameters, such as tricuspid annular plane systolic excursion, pulmonary artery acceleration time, RV internal diameter, RV myocardial performance index, and cardiac output determined by echocardiography (Figure XIXB in the online-only Data Supplement). In contrast, sanguinarine did not change LV systolic pressure and LV end diastolic pressure determined by catheter or LV ejection fraction determined by echocardiography (Figure XIXA and B in the online-only Data Supplement). Finally, sanguinarine treatment significantly improved exercise capacity assessed by a treadmill walking distance (Figure 8J). Next, we prepared a mouse model of Sugen/hypoxia-induced PH using SMC-*Sepp1*$^{-/-}$ mice, which were treated with sanguinarine to further evaluate the contribution of SeP-mediated therapeutic effects. Consistent with the

Figure 7 Continued. J, Quantification of GSH/GSSG ratio in *Sepp1*$^{+/+}$ and *Sepp1*$^{-/-}$ PASMCs after exposure to normoxia (21% O_2) or hypoxia (1% O_2) for 4 hours (n=8 each). **K**, Quantification of oxygen consumption rate (OCR) of PAH-PASMCs and control PASMCs under normoxia (21% O_2) or hypoxia (1% O_2) for 4 hours (n=5 each). Oligomycin inhibits ATP synthase (complex V) and the decrease in OCR, followed by oligomycin correlates to the mitochondrial respiration associated with cellular ATP production. Carbonyl cyanide-4 (trifluoromethoxy) phenylhydrazone (FCCP) is an uncoupling agent that disrupts the mitochondrial membrane potential. As a result, electron flow through the electron transport chain is uninhibited and oxygen is maximally consumed by complex IV. Rotenone and antimycin A were injected to inhibit the flux of electrons through complexes I and III, respectively, and thus shut down mitochondrial oxygen consumption. **L**, Quantification of the OCR/ECAR (extracellular acidification rate, a surrogate for glycolysis) ratio in PAH-PASMCs and control PASMCs under normoxia (21% O_2) or hypoxia (1% O_2) for 4 hours (n=5 each). **M**, **Left,** Representative images of PAH-PASMCs and control PASMCs labeled for mitochondria. Nuclei were counterstained using DAPI (4′,6-diamidino-2-phenylindole). Scale bars, 20 μm. **Right,** Representative transmission electron microscopy (TEM) images of PAH-PASMCs and control PASMCs. Scale bars, 2 μm. **N**, Quantification of OCR of *Sepp1*$^{+/+}$ and *Sepp1*$^{-/-}$ PASMCs under normoxia (21% O_2) or hypoxia (1% O_2) for 4 hours (n=5 each). **O**, Quantification of the OCR/ECAR ratio in *Sepp1*$^{+/+}$ and *Sepp1*$^{-/-}$ PASMCs under normoxia (21% O_2) or hypoxia (1% O_2) for 4 hours (n=5 each). **P**, **Left,** Representative images of *Sepp1*$^{+/+}$ and *Sepp1*$^{-/-}$ PASMCs labeled for mitochondria. Nuclei were counterstained using DAPI. Scale bars, 20 μm. **Right,** Representative TEM images of *Sepp1*$^{+/+}$ and *Sepp1*$^{-/-}$ PASMCs. Scale bars, 2 μm. Data represent the mean±SEM throughout. **P*<0.05. Comparisons of parameters were performed with 2-way ANOVA, followed by Tukey's honestly significant difference test for multiple comparisons. si indicates small interfering.

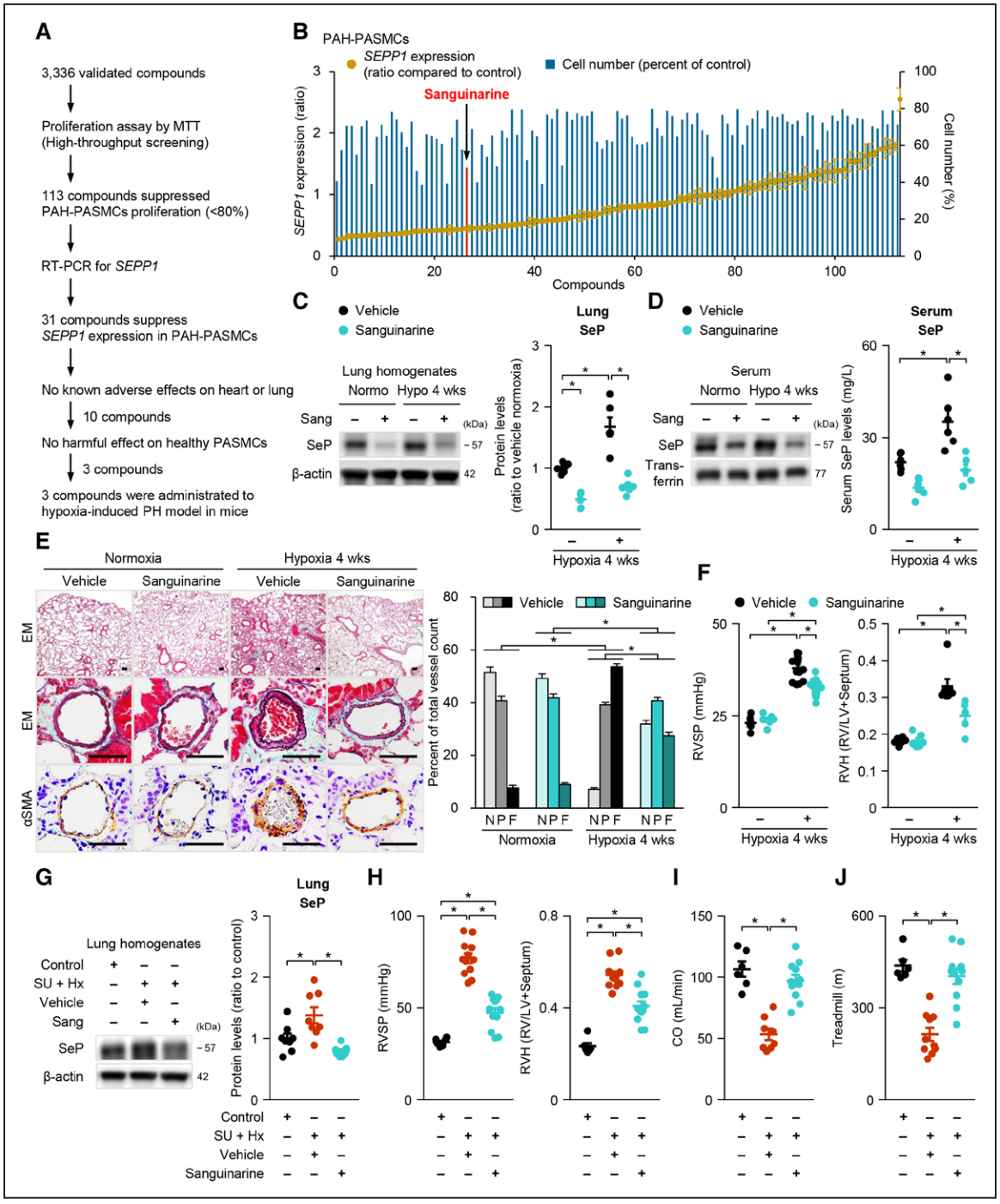

Figure 8. Sanguinarine ameliorates PH in animal models in vivo.

A, Schematic outline of high-throughput screening to identify compounds that suppress *SEPP1* expression and proliferation in pulmonary arterial hypertension (PAH)–pulmonary artery smooth muscle cells (PASMCs). First, we treated PAH-PASMCs with 3336 compounds (5 μmol/L each) for 48 hours and performed a proliferation assay (MTT assay). We identified 113 compounds that suppressed PAH-PASMCs proliferation by >20%. We then treated PAH-PASMCs with these 113 compounds (5 μmol/L each) for 4 hours, extracted total RNA to measure the selenoprotein P (SeP) expression by RT-PCR, and found 31 compounds that suppress *SEPP1* mRNA. We excluded compounds with known adverse effects on the heart or lungs and those producing harmful effects on control PASMCs. Finally, we selected 3 compounds for administration in hypoxia-induced pulmonary hypertension (PH) in mice. MTT, 3-(4,5-di-methylthiazol-2-yl)-2,5-diphenyltetrazolium bromide. **B**, Results of the 113 compounds that suppress PAH-PASMC proliferation (blue bars) and *SEPP1* gene expression (brown plots). **C**, Representative Western blots and quantification of SeP protein levels in the lungs with or without sanguinarine treatment (5 mg/kg/day) under normoxia or hypoxia (10% O_2) for 4 weeks (n=6 each). **D**, Representative Western blots and quantification of SeP protein levels in the serum with or without sanguinarine treatment under normoxia or hypoxia (10% O_2) for 4 weeks (n=6 each). **E**, **Left,** Representative Elastica-Masson (EM) and immunostainings for α–smooth muscle actin (αSMA) of the distal pulmonary arteries. Scale bars, 50 μm. **Right,** Muscularization of the distal pulmonary arteries with a diameter of 20 to 70 μm in mice exposed to normoxia (n=6 each) or hypoxia for 4 weeks (n=15 each). N, nonmuscularized vessels; P, partially muscularized vessels; F, fully muscularized vessels. **F**, Right ventricular (RV) systolic pressure (RVSP, **left**) and right ventricular hypertrophy (RVH, **right**) in mice with or without sanguinarine treatment under normoxia (n=6 each) or hypoxia (10% O_2) for 4 weeks (n=13–14 in RVSP, n=7 in RVH). **G**, Representative Western blots and quantification of SeP protein levels in the lungs of normoxia controls or rats exposed to chronic hypoxia for 21 days in combination with the VEGF receptor blocker, SU5416 (Sugen/hypoxia rats), (*Continued*)

results in the rat model of Sugen/hypoxia-induced PH, sanguinarine treatment significantly improved the hemodynamic parameters, RV function, and exercise capacity in the SMC-*Sepp1*$^{+/+}$ Sugen/hypoxia (control) mice (Figure XXA through C in the online-only Data Supplement). In contrast, SMC-*Sepp1*$^{-/-}$ Sugen/hypoxia mice showed significant amelioration of PH compared with controls. Additionally, sanguinarine treatment did not show further improvements in SMC-*Sepp1*$^{-/-}$ mice (Figure XXA through C in the online-only Data Supplement). These findings strengthen the SeP-mediated development of Sugen/hypoxia-induced PH and the sanguinarine-mediated amelioration of PH. Consistently, sanguinarine treatment significantly reduced proliferation of *Sepp1*$^{+/+}$ PASMCs to a similar level in *Sepp1*$^{-/-}$ PASMCs. In contrast, proliferation of *Sepp1*$^{-/-}$ PASMCs was not affected by sanguinarine treatment (Figure XXD in the online-only Data Supplement). These results suggest that sanguinarine suppresses SeP in the lungs and ameliorates PH and RV failure in different animal models of PH.

DISCUSSION

The present study demonstrates that upregulation of SeP in PASMCs is a novel pathological change in PAH that induces proliferation, enhanced oxidative stress, and mitochondrial dysfunction in PASMCs. The present study also suggests the novel strategy of SeP inhibition in PASMCs to prevent the development of PH. These concepts are based on the following findings: (1) SeP was upregulated in PAH-PASMCs; (2) 5 genetically modified mice showed a critical role for SeP in PASMCs in the development of hypoxia-induced PH; (3) higher SeP in PAH-PASMCs induced HIF-1α upregulation, FOXO3a inactivation, a reduced GSH/GSSG ratio, increased oxidative stress, and mitochondrial dysfunction, resulting in excessive proliferation of PAH-PASMCs; and (4) sanguinarine reduced SeP expression and PASMC proliferation, as well as ameliorated PH in animal models of different mechanisms.

SeP as a Novel Pathogenic Protein in the Pathogenesis of PAH

Because there is a limited efficacy in the treatment of patients with severe PAH, we performed a series of screening to find a novel therapeutic target. After the rigorous analyses of microarray screening with PAH-PASMCs, we finally focused on SeP as a pathogenic protein in PAH. As demonstrated in the present study, SeP is a secreted protein that promotes PASMC proliferation. Although it has been shown that 60% of serum SeP is produced by hepatocytes in the physiological condition,[26] SeP is also expressed in many types of cells for secretion.[33,68,69] Indeed, we demonstrated that SeP is highly upregulated in the distal pulmonary arteries of patients with PAH. Our findings suggest that the upregulation of SeP in PAH-PASMCs is a trigger as well as a promoter for the development of PAH. We also demonstrated a synergistic interaction among SeP, HIF-1α, and FOXO3a in PAH-PASMCs through extracellular SeP-ApoER2 signaling. Thus, SeP-mediated PASMC proliferation may mechanistically involve HIF-1α–mediated mitochondrial dysfunction, similar to cancer cells.[70] Indeed, activated HIF-1α in normoxia is well known in PAH-PASMCs. It induces transcription of many genes producing proproliferative and antiapoptotic signals, impaired oxidative glucose metabolism, and the shift to aerobic glycolysis.[71] In contrast, under physiological conditions, activated HIF-1α stimulates FOXO3a,[16] which promotes cellular adaptation to hypoxic stress, suppresses survival signals, and induces apoptosis.[72,73] Thus, the complex interaction between HIF-1α and FOXO3a is substantially involved in the fine control of cellular homeostasis and pathological adaptation.[74] In PAH-PASMCs, we found that the expression of SeP and HIF-1α affected each other, which accompanied SeP-mediated activation of Akt, ERK1/2, and resultant FOXO3a phosphorylation and degradation. These findings suggest that excessive SeP disrupts the fine tuning of intracellular homeostasis between HIF-1α and FOXO3a, which induces constitutive activation of HIF-1α and mitochondrial dysfunction in PAH-PASMCs. Additionally, we found that serum levels of selenium were increased in patients with PAH, suggesting that SeP function as a selenium supplier is preserved in patients with PAH. In the present study, overexpression of Mut-P, which has no selenium, also increased ROS levels and reduced GSH in control PASMCs, which was similar to the effect by overexpression of intact SeP. Indeed, it has been reported that SeP possesses 2 functions: enzyme activity in the N-terminal region and selenium-supply activity in the C-terminal region.[75] Additionally, ApoER2 is a candidate receptor for SeP in PAH-PASMCs and activates intracellular signaling pathways.[76] Altogether, our findings on selenium status in patients with PAH and previous reports indicate that SeP-mediated development of PAH is independent of its selenium supply.

Figure 8 Continued. followed by treatment with vehicle or sanguinarine via gavage during 28 days after induction of PAH (n=8 each). **H**, RVSP (**left**) and RVH (**right**) in Sugen/hypoxia rats by treatment with vehicle or sanguinarine via gavage during 28 days after induction of PAH (n=6 for control rats that did not receive SU5416 injection or chronic hypoxia; n=12 for vehicle or sanguinarine-treated rats per group). **I**, Cardiac output (CO) in Sugen/hypoxia rats by treatment with vehicle or sanguinarine via gavage during 28 days after induction of PAH (n=6 for control, n=8 for vehicle, and n=11 for sanguinarine-treated rats per group). **J**, Walking distance assessed by a treadmill test (n=6 for control and n=12 for vehicle- or sanguinarine-treated rats per group). Data represent the mean±SEM. *P<0.05. Comparisons of parameters were performed with 1- or 2-way ANOVA, followed by Tukey's honestly significant difference test for multiple comparisons. Hypo indicates hypoxia; LV, left ventricle; Normo, normoxia; Sang, sanguinarine; and SU + Hx, Sugen/hypoxia.

SeP Enhances Oxidative Stress in PAH-PASMCs

Mounting evidence provides insights into the role of oxidative stress in the pathogenesis of PAH.[77] Animal models of PH show increased oxidative stress and decreased antioxidant levels, both of which promote PASMC proliferation, pulmonary vascular remodeling, and RV failure.[78] One of the mechanisms for the enhanced production of ROS in PAH-PASMCs is an excessive activation of NADPH oxidases.[79] The activation of NADPH oxidases increases ROS generation, promotes PASMC hyperplasia and hypertrophy, and contributes to the transcription and stabilization of HIF-1α.[80] Additionally, the cellular redox status depends on the balance between oxidized and reduced forms of intracellular redox molecules, in which GSH plays a crucial role. Because protein levels of GSH in quiescent cells are much higher than those of GSSG, oxidation of GSH and conversion to GSSG will dramatically decrease the GSH/GSSG ratio and significantly change the cellular redox status. Both changes in the redox potential because of the decrease in the GSH/GSSG ratio and the generation of ROS can induce the formation of mixed disulfides between cysteine residues of some proteins and GSH.[81] According to this mechanism induced by a decreased GSH/GSSG ratio and increased ROS, the GSH adducts on HIF-1α Cys^{520} inhibit its degradation and stabilize the transcription factor, with a resultant increase in target gene expression.[82] In PAH-PASMCs, the mechanisms for their apoptosis resistance and excessive proliferation can be explained by normoxic activation of HIF-1α (pseudohypoxic environment)[22] and the resultant metabolic shift toward glycolytic metabolism, and downregulation of mitochondrial glucose oxidation (Warburg effect).[19] In the present study, we found that the enhanced expression of SeP reduced the GSH/GSSH ratio and increased oxidative stress levels, contributing to the enhanced expression and stabilization of HIF-1α even in normoxia, and these changes had no relation to selenium content in SeP. In addition to these findings, we found that *Sepp1*$^{-/-}$ PASMCs had an increased GSH/GSSG ratio, reduced ROS levels, and reduced HIF-1α levels in both normoxia and hypoxia. These results suggest that SeP, even without its selenium content, acts as an upstream negative regulator of antioxidative stress signaling, which both induces ROS generation through NADPH oxidases and stabilizes HIF-1α, providing a potential mechanism of SeP-mediated HIF-1α activation and resultant proliferation of PASMCs and their survival in PAH.

SeP Causes Metabolic Shift in PAH-PASMCs

Dysregulated mitochondrial function in PAH-PASMCs causes a decrease in the production of mROS with a resultant normoxic activation of HIF-1α, which induces pyruvate dehydrogenase kinase, impairs mitochondrial respiration and glucose oxidation, and promotes a glycolytic metabolic state.[22] This metabolic shift impairs the function of the mitochondrial electron transport chain further, which reduces mROS in PAH-PASMCs.[83] Moreover, reduced levels of mROS inhibit the Kv channel and increase intracellular calcium concentration, which augments PASMC constriction.[78,84] Thus, a metabolic shift toward glycolytic metabolism and downregulation of mitochondrial glucose oxidation in PAH-PASMCs will contribute to their apoptosis resistance and excessive proliferation.[19] Our present findings support all of these pathological changes in PAH-PASMCs as follows: (1) PAH-PASMCs exhibited a decrease in de novo synthesis of GSH, (2) PAH-PASMCs had lower levels of GSH/GSSG ratio and increased levels of ROS generated by NADPH oxidases compared with control PASMCs, (3) PAH-PASMCs had increased levels of HIF-1α and mitochondrial fragmentation, (4) PAH-PASMCs had lower levels of maximal OCR and the OCR/ECAR ratio compared with control PASMCs with a resultant increase in mitochondrial membrane potential ($\Delta\Psi$m) and decrease in mROS production, and (5) *Sepp1*$^{-/-}$ PASMCs showed an increased GSH/GSSG ratio, lower ROS, increased mitochondrial network, and increased mitochondrial energy metabolism compared with *Sepp1*$^{+/+}$ PASMCs. These findings suggest a possible mechanism that excessive SeP reduces GSH, whereas it increases GSSG production, upregulates ROS production by NADPH oxidases, and stabilizes HIF-1α even under normoxic conditions, contributing to the pseudohypoxic state, mitochondrial dysfunction, and excessive proliferation/apoptosis-resistance in PAH-PASMCs.

Study Limitations

Several limitations should be mentioned for the present study. First, although we found a 32-fold increase of SeP in PAH-PASMCs compared with control PASMCs, the underlying mechanisms for it remain to be elucidated. It is established and we have confirmed that the activities of NADPH oxidases and resultant oxidative stress levels are significantly higher in PAH-PASMCs.[22] In contrast, SeP is important for selenium homeostasis, where SeP with a selenocysteine amino acid residue plays a crucial role in cellular homeostasis.[26] Functionally characterized selenoproteins consist of 5 GPx and 3 thioredoxin reductases, all of which contain 1 selenocysteine.[27] Here, GPx is an enzyme family with peroxidase activity, which serves to protect cells from oxidative damage.[31] When we consider the roles of selenoproteins, upregulation of SeP in PAH-PASMCs can be explained, at least in part, by cellular responses to protect the cells against excessive oxidative stress. Indeed, we found that serum selenium levels were significantly increased in patients with PAH. Here,

it was previously demonstrated that SeP has bifunctional enzyme activities in the N-terminal region and selenium-supply activity in the C-terminal region.[75] Moreover, it is also known that ApoER2, 1 of the receptors for SeP, uptakes extracellular SeP and activates intracellular signaling.[76] In the present study, overexpression of Mut-P (SeP without any selenium) increased ROS levels and reduced GSH in control PASMCs. Altogether, these findings and previous reports suggest that upregulated SeP in PAH-PASMCs promotes the development of PAH independently from its selenium supply. Thus, in addition to the traditionally known roles as a cargo for selenium, SeP protein may have other functions, including an inhibitory effect on GSH, resulting in increased oxidative stress, excessive proliferation, and apoptosis resistance in PAH-PASMCs. Second, the beneficial effects of sanguinarine may involve mechanisms other than reducing SeP. Indeed, sanguinarine regulates several intracellular molecules, including signal transducer and activator of transcription, STAT3.[67] Thus, sanguinarine may ameliorate PH by reducing SeP and by other mechanisms.

CONCLUSIONS

PAH is a rare disease, with an estimated prevalence of 52 cases per million.[85] However, the prevalence of PAH is rapidly increasing along with medical awareness and is much higher in patients with lung disease, congenital heart disease, collagen disease, and infectious disorders.[5] Moreover, it is estimated that the prevalence of PH is about 1% of the general population, which increases to 10% of individuals >65 years of age.[5] Over the past 20 years, substantial efforts have been made to develop effective therapies for patients with PAH.[86] However, we still have limited therapeutic strategies, and no established treatments are available for most patients with PAH.[86] Because conventional pulmonary vasodilators have limited efficacy for the treatment of severe PAH, we have performed a series of screens and found a novel therapeutic target, SeP. As shown in the present study, SeP promoted PASMC proliferation, which prompted us to find an SeP inhibitor as a novel therapy for PAH. At this point, we have no drugs available for targeting PASMC proliferation[86] and a limited report of SeP targeting, in which metformin may suppress its expression in the liver via AMPK activation.[87] Coincidentally, we have recently demonstrated that endothelial AMPK plays a crucial role in suppressing the development of hypoxia-induced PH, which can be achieved with metformin.[35] However, metformin has no effect on the expression of SeP in PAH-PASMCs (unpublished data). Moreover, we performed *in silico* screening and found no compound with an inhibitory effect on SeP. Thus, we performed a high-throughput screening of small molecules and identified an orally active small molecule, sanguinarine. It has been reported that oral sanguinarine administration successfully inhibited tumor growth.[67] When we consider the proproliferative role of SeP in PAH-PASMCs, the antiproliferative effect of sanguinarine in several kinds of cancer in vivo could be attributed to the suppression of SeP.[67] Actually, in the present study, sanguinarine administration to the animal models of PH revealed therapeutic effects on PH and RV failure without any adverse effects.

In the present study, we demonstrated that SeP is a secreted protein that promotes PASMC proliferation. Moreover, serum levels of SeP were significantly elevated in patients with PAH, in whom higher serum levels of SeP predicted a poor outcome. Conversely, treatment with SeP inhibitors reduced protein levels of SeP and ameliorated PH. Based on these results, serum levels of SeP can be used as a novel biomarker for PAH and are useful to evaluate the therapeutic effect of SeP inhibitors (companion diagnostics). Using a combination of SeP inhibitors and serum levels of SeP, we may find good candidates among patients with PAH who can be used to demonstrate the effectiveness of this strategy. By targeting SeP, we will promote translational research and develop early diagnostics and novel therapeutic agents for the treatment of patients with PAH.

In conclusion, SeP is a crucial molecule in the pathogenesis of PAH and is useful as a novel biomarker and therapeutic target of the disorder.

ARTICLE INFORMATION

Received December 6, 2017; accepted March 28, 2018.

The online-only Data Supplement is available with this article at https://www.ahajournals.org/doi/suppl/10.1161/CIRCULATIONAHA.117.033113.

Correspondence

Hiroaki Shimokawa, MD, PhD, Department of Cardiovascular Medicine, Tohoku University Graduate School of Medicine, 1-1 Seiryo-machi, Aoba-ku, Sendai 980–8574, Japan. E-mail shimo@cardio.med.tohoku.ac.jp

Affiliations

Department of Cardiovascular Medicine, Tohoku University Graduate School of Medicine, Sendai, Japan (N.K., K.S., R.K., S.M., N.Y., M.E.-A.-M., M.A.H.S., J.O., T.S., M.N., S.S., H.S.). Research Fellow of Japan Society for the Promotion of Science, Tokyo (N.K., R.K.). Department of Medical Life Systems, Faculty of Life and Medical Sciences, Doshisha University, Kyotanabe, Japan (Y.S.). Department of Thoracic Surgery, Institute of Development, Aging, and Cancer, Tohoku University, Sendai, Japan (Y.H., Y.O.).

Acknowledgments

We are grateful to the laboratory members in the Department of Cardiovascular Medicine at Tohoku University for valuable technical assistance, especially Yumi Watanabe, Ai Nishihara, and Hiromi Yamashita. We thank Drs Hill and Burk for providing us with *Sepp1* knockout mice and conditional *Sepp1* knockout mice, and Dr Motohashi for the fruitful and constructive discussion. Drs Kikuchi, K. Satoh, and Shimokawa designed the study. Drs Kikuchi, K. Satoh, Kurosawa, Elias-Al-Mamun, Siddique, Omura, T. Satoh, Nogi, Sunamura, and Yaoita performed the experiments. Drs Kikuchi, K. Satoh, and Miyata analyzed the data. Drs Saito, Hoshikawa, and Okada. provided the resources. Drs Kikuchi, K. Satoh, and Shimokawa wrote the manuscript.

Sources of Funding

This work was partially supported by the Platform Project for Supporting Drug Discovery and Life Science Research from the Japan Agency for Medical Research and Development. This work was also supported in part by the grants-in-aid for Scientific Research (15H02535, 15H04816, and 15K15046), all of which are from the Ministry of Education, Culture, Sports, Science, and Technology, Tokyo, Japan; grants-in-aid for Scientific Research from the Ministry of Health, Labor, and Welfare, Tokyo, Japan (10102895); and grants-in-aid for Scientific Research from the Japan Agency for Medical Research and Development, Tokyo, Japan (15ak0101035h0001, 16ek0109176h0001, and 17ek0109227h0001).

Disclosures

None.

REFERENCES

1. Morrell NW, Adnot S, Archer SL, Dupuis J, Jones PL, MacLean MR, McMurtry IF, Stenmark KR, Thistlethwaite PA, Weissmann N, Yuan JX, Weir EK. Cellular and molecular basis of pulmonary arterial hypertension. *J Am Coll Cardiol*. 2009;54(1 suppl):S20–S31. doi: 10.1016/j.jacc.2009.04.018.
2. Rabinovitch M. Molecular pathogenesis of pulmonary arterial hypertension. *J Clin Invest*. 2012;122:4306–4313. doi: 10.1172/JCI60658.
3. Austin ED, Loyd JE. The genetics of pulmonary arterial hypertension. *Circ Res*. 2014;115:189–202. doi: 10.1161/CIRCRESAHA.115.303404.
4. Kholdani C, Fares WH, Mohsenin V. Pulmonary hypertension in obstructive sleep apnea: is it clinically significant? A critical analysis of the association and pathophysiology. *Pulm Circ*. 2015;5:220–227. doi: 10.1086/679995.
5. Hoeper MM, Humbert M, Souza R, Idrees M, Kawut SM, Sliwa-Hahnle K, Jing Z-C, Gibbs JSR. A global view of pulmonary hypertension. *Lancet Respir Med*. 2016;4:306–322. doi: 10.1016/s2213-2600(15)00543-3.
6. Jiang X, Yuan L, Li P, Wang J, Wang P, Zhang L, Sun B, Sun W. Effect of simvastatin on 5-HT and 5-HTT in a rat model of pulmonary artery hypertension. *Cell Physiol Biochem*. 2015;37:1712–1724. doi: 10.1159/000438536.
7. Grunig G, Marsh LM, Esmaeil N, Jackson K, Gordon T, Reibman J, Kwapiszewska G, Park SH. Perspective: ambient air pollution: inflammatory response and effects on the lung's vasculature. *Pulm Circ*. 2014;4:25–35. doi: 10.1086/674902.
8. Ventetuolo CE, Baird GL, Barr RG, Bluemke DA, Fritz JS, Hill NS, Klinger JR, Lima JA, Ouyang P, Palevsky HI, Palmisciano AJ, Krishnan I, Pinder D, Preston IR, Roberts KE, Kawut SM. Higher estradiol and lower dehydroepiandrosterone-sulfate levels are associated with pulmonary arterial hypertension in men. *Am J Respir Crit Care Med*. 2016;193:1168–1175. doi: 10.1164/rccm.201509-1785OC.
9. Chen X, Talati M, Fessel JP, Hemnes AR, Gladson S, French J, Shay S, Trammell A, Phillips JA, Hamid R, Cogan JD, Dawson EP, Womble KE, Hedges LK, Martinez EG, Wheeler LA, Loyd JE, Majka SJ, West J, Austin ED. Estrogen metabolite 16α-hydroxyestrone exacerbates bone morphogenetic protein receptor type II-associated pulmonary arterial hypertension through microRNA-29-mediated modulation of cellular metabolism. *Circulation*. 2016;133:82–97. doi: 10.1161/CIRCULATIONAHA.115.016133.
10. Irwin DC, Garat CV, Crossno JT Jr, MacLean PS, Sullivan TM, Erickson PF, Jackman MR, Harral JW, Reusch JE, Klemm DJ. Obesity-related pulmonary arterial hypertension in rats correlates with increased circulating inflammatory cytokines and lipids and with oxidant damage in the arterial wall but not with hypoxia. *Pulm Circ*. 2014;4:638–653. doi: 10.1086/678510.
11. Perros F, Günther S, Ranchoux B, Godinas L, Antigny F, Chaumais MC, Dorfmüller P, Hautefort A, Raymond N, Savale L, Jaïs X, Girerd B, Cottin V, Sitbon O, Simonneau G, Humbert M, Montani D. Mitomycin-induced pulmonary veno-occlusive disease: evidence from human disease and animal models. *Circulation*. 2015;132:834–847. doi: 10.1161/CIRCULATIONAHA.115.014207.
12. Gatzoulis MA, Beghetti M, Landzberg MJ, Galiè N. Pulmonary arterial hypertension associated with congenital heart disease: recent advances and future directions. *Int J Cardiol*. 2014;177:340–347. doi: 10.1016/j.ijcard.2014.09.024.
13. Chung L, Liu J, Parsons L, Hassoun PM, McGoon M, Badesch DB, Miller DP, Nicolls MR, Zamanian RT. Characterization of connective tissue disease-associated pulmonary arterial hypertension from REVEAL: identifying systemic sclerosis as a unique phenotype. *Chest*. 2010;138:1383–1394. doi: 10.1378/chest.10-0260.
14. Rich JD, Rich S. Clinical diagnosis of pulmonary hypertension. *Circulation*. 2014;130:1820–1830. doi: 10.1161/CIRCULATIONAHA.114.006971.
15. Austin ED, West J, Loyd JE, Hemnes AR. Translational advances in the field of pulmonary hypertension molecular medicine of pulmonary arterial hypertension: from population genetics to precision medicine and gene editing. *Am J Respir Crit Care Med*. 2017;195:23–31. doi: 10.1164/rccm.201605-0905PP.
16. Bakker WJ, Harris IS, Mak TW. FOXO3a is activated in response to hypoxic stress and inhibits HIF1-induced apoptosis via regulation of CITED2. *Mol Cell*. 2007;28:941–953. doi: 10.1016/j.molcel.2007.10.035.
17. Boucherat O, Vitry G, Trinh I, Paulin R, Provencher S, Bonnet S. The cancer theory of pulmonary arterial hypertension. *Pulm Circ*. 2017;7:285–299. doi: 10.1177/2045893217701438.
18. Pullamsetti SS, Savai R, Seeger W, Goncharova EA. Translational advances in the field of pulmonary hypertension: from cancer biology to new pulmonary arterial hypertension therapeutics: targeting cell growth and proliferation signaling hubs. *Am J Respir Crit Care Med*. 2017;195:425–437. doi: 10.1164/rccm.201606-1226PP.
19. Archer SL. Mitochondrial dynamics–mitochondrial fission and fusion in human diseases. *N Engl J Med*. 2013;369:2236–2251. doi: 10.1056/NEJMra1215233.
20. Ryan JJ, Archer SL. Emerging concepts in the molecular basis of pulmonary arterial hypertension: part I: metabolic plasticity and mitochondrial dynamics in the pulmonary circulation and right ventricle in pulmonary arterial hypertension. *Circulation*. 2015;131:1691–1702. doi: 10.1161/CIRCULATIONAHA.114.006979.
21. Sancho P, Barneda D, Heeschen C. Hallmarks of cancer stem cell metabolism. *Br J Cancer*. 2016;114:1305–1312. doi: 10.1038/bjc.2016.152.
22. Sutendra G, Michelakis ED. The metabolic basis of pulmonary arterial hypertension. *Cell Metabolism*. 2014;19:558–573. doi: 10.1016/j.cmet.2014.01.004.
23. West J, Niswender KD, Johnson JA, Pugh ME, Gleaves L, Fessel JP, Hemnes AR. A potential role for insulin resistance in experimental pulmonary hypertension. *Eur Respir J*. 2013;41:861–871. doi: 10.1183/09031936.00030312.
24. Hansmann G, Wagner RA, Schellong S, Perez VA, Urashima T, Wang L, Sheikh AY, Suen RS, Stewart DJ, Rabinovitch M. Pulmonary arterial hypertension is linked to insulin resistance and reversed by peroxisome proliferator-activated receptor-gamma activation. *Circulation*. 2007;115:1275–1284. doi: 10.1161/CIRCULATIONAHA.106.663120.
25. Shimokawa H, Sunamura S, Satoh K. RhoA/Rho-kinase in the cardiovascular system. *Circ Res*. 2016;118:352–366. doi: 10.1161/CIRCRESAHA.115.306532.
26. Hill KE, Wu S, Motley AK, Stevenson TD, Winfrey VP, Capecchi MR, Atkins JF, Burk RF. Production of selenoprotein P (Sepp1) by hepatocytes is central to selenium homeostasis. *J Biol Chem*. 2012;287:40414–40424. doi: 10.1074/jbc.M112.421404.
27. Burk RF, Hill KE. Selenoprotein P: an extracellular protein with unique physical characteristics and a role in selenium homeostasis. *Annu Rev Nutr*. 2005;25:215–235. doi: 10.1146/annurev.nutr.24.012003.132120.
28. Hill KE, Zhou J, McMahan WJ, Motley AK, Atkins JF, Gesteland RF, Burk RF. Deletion of selenoprotein P alters distribution of selenium in the mouse. *J Biol Chem*. 2003;278:13640–13646. doi: 10.1074/jbc.M300755200.
29. Saito Y, Takahashi K. Characterization of selenoprotein P as a selenium supply protein. *Eur J Biochem*. 2002;269:5746–5751.
30. Tujebajeva RM, Harney JW, Berry MJ. Selenoprotein P expression, purification, and immunochemical characterization. *J Biol Chem*. 2000;275:6288–6294.
31. Rayman MP. The importance of selenium to human health. *Lancet*. 2000;356:233–241. doi: 10.1016/S0140-6736(00)02490-9.
32. Misu H, Takamura T, Takayama H, Hayashi H, Matsuzawa-Nagata N, Kurita S, Ishikura K, Ando H, Takeshita Y, Ota T, Sakurai M, Yamashita T, Mizukoshi E, Yamashita T, Honda M, Miyamoto K, Kubota T, Kubota N, Kadowaki T, Kim HJ, Lee IK, Minokoshi Y, Saito Y, Takahashi K, Yamada Y, Takakura N, Kaneko S. A liver-derived secretory protein, selenoprotein P, causes insulin resistance. *Cell Metab*. 2010;12:483–495. doi: 10.1016/j.cmet.2010.09.015.
33. Strauss E, Oszkinis G, Staniszewski R. SEPP1 gene variants and abdominal aortic aneurysm: gene association in relation to metabolic risk factors and peripheral arterial disease coexistence. *Sci Rep*. 2014;4:7061. doi: 10.1038/srep07061.
34. Satoh K, Satoh T, Kikuchi N, Omura J, Kurosawa R, Suzuki K, Sugimura K, Aoki T, Nochioka K, Tatebe S, Miyamichi-Yamamoto S, Miura M, Shimizu T, Ikeda S, Yaoita N, Fukumoto Y, Minami T, Miyata S, Nakamura

K, Ito H, Kadomatsu K, Shimokawa H. Basigin mediates pulmonary hypertension by promoting inflammation and vascular smooth muscle cell proliferation. *Circ Res*. 2014;115:738–750. doi: 10.1161/CIRCRESAHA.115.304563.
35. Omura J, Satoh K, Kikuchi N, Satoh T, Kurosawa R, Nogi M, Otsuki T, Kozu K, Numano K, Suzuki K, Sunamura S, Tatebe S, Aoki T, Sugimura K, Miyata S, Hoshikawa Y, Okada Y, Shimokawa H. Protective roles of endothelial AMP-activated protein kinase against hypoxia-induced pulmonary hypertension in mice. *Circ Res*. 2016;119:197–209. doi: 10.1161/CIRCRESAHA.115.308178.
36. Kim YM, Haghighat L, Spiekerkoetter E, Sawada H, Alvira CM, Wang L, Acharya S, Rodriguez-Colon G, Orton A, Zhao M, Rabinovitch M. Neutrophil elastase is produced by pulmonary artery smooth muscle cells and is linked to neointimal lesions. *Am J Pathol*. 2011;179:1560–1572. doi: 10.1016/j.ajpath.2011.05.051.
37. Alastalo TP, Li M, Perez Vde J, Pham D, Sawada H, Wang JK, Koskenvuo M, Wang L, Freeman BA, Chang HY, Rabinovitch M. Disruption of PPARγ/β-catenin-mediated regulation of apelin impairs BMP-induced mouse and human pulmonary arterial EC survival. *J Clin Invest*. 2011;121:3735–3746. doi: 10.1172/JCI43382.
38. Comhair SA, Xu W, Mavrakis L, Aldred MA, Asosingh K, Erzurum SC. Human primary lung endothelial cells in culture. *Am J Respir Cell Mol Biol*. 2012;46:723–730. doi: 10.1165/rcmb.2011-0416TE.
39. Shimizu T, Fukumoto Y, Tanaka S, Satoh K, Ikeda S, Shimokawa H. Crucial role of ROCK2 in vascular smooth muscle cells for hypoxia-induced pulmonary hypertension in mice. *Arterioscler Thromb Vasc Biol*. 2013;33:2780–2791. doi: 10.1161/ATVBAHA.113.301357.
40. Tusher VG, Tibshirani R, Chu G. Significance analysis of microarrays applied to the ionizing radiation response. *Proc Natl Acad Sci U S A*. 2001;98:5116–5121. doi: 10.1073/pnas.091062498.
41. Bonnet S, Provencher S, Guignabert C, Perros F, Boucherat O, Schermuly RT, Hassoun PM, Rabinovitch M, Nicolls MR, Humbert M. Translating research into improved patient care in pulmonary arterial hypertension. *Am J Respir Crit Care Med*. 2017;195:583–595. doi: 10.1164/rccm.201607-1515PP.
42. Vitali SH, Hansmann G, Rose C, Fernandez-Gonzalez A, Scheid A, Mitsialis SA, Kourembanas S. The sugen 5416/hypoxia mouse model of pulmonary hypertension revisited: long-term follow-up. *Pulm Circ*. 2014;4:619–629. doi: 10.1086/678508.
43. Satoh K, Fukumoto Y, Nakano M, Sugimura K, Nawata J, Demachi J, Karibe A, Kagaya Y, Ishii N, Sugamura K, Shimokawa H. Statin ameliorates hypoxia-induced pulmonary hypertension associated with down-regulated stromal cell-derived factor-1. *Cardiovasc Res*. 2009;81:226–234. doi: 10.1093/cvr/cvn244.
44. Satoh K, Kagaya Y, Nakano M, Ito Y, Ohta J, Tada H, Karibe A, Minegishi N, Suzuki N, Yamamoto M, Ono M, Watanabe J, Shirato K, Ishii N, Sugamura K, Shimokawa H. Important role of endogenous erythropoietin system in recruitment of endothelial progenitor cells in hypoxia-induced pulmonary hypertension in mice. *Circulation*. 2006;113:1442–1450. doi: 10.1161/CIRCULATIONAHA.105.583732.
45. Hill KE, Zhou J, McMahan WJ, Motley AK, Burk RF. Neurological dysfunction occurs in mice with targeted deletion of the selenoprotein P gene. *J Nutr*. 2004;134:157–161. doi: 10.1093/jn/134.1.157.
46. Satoh T, Satoh K, Yaoita N, Kikuchi N, Omura J, Kurosawa R, Numano K, Al-Mamun E, Siddique MA, Sunamura S, Nogi M, Suzuki K, Miyata S, Morser J, Shimokawa H. Activated TAFI promotes the development of chronic thromboembolic pulmonary hypertension: a possible novel therapeutic target. *Circ Res*. 2017;120:1246–1262. doi: 10.1161/CIRCRESAHA.117.310640.
47. Elias-Al-Mamun M, Satoh K, Tanaka S, Shimizu T, Nergui S, Miyata S, Fukumoto Y, Shimokawa H. Combination therapy with fasudil and sildenafil ameliorates monocrotaline-induced pulmonary hypertension and survival in rats. *Circ J*. 2014;78:967–976. doi: 10.1253/circj.CJ-13–1174.
48. Breiman L, Friedman JH, Olshen RA, Stone CJ. *Classification and Regression Trees*. Monterey, CA: Wadsworth and Brooks; 1984.
49. van der Vos KE, Coffer PJ. The extending network of FOXO transcriptional target genes. *Antioxid Redox Signal*. 2011;14:579–592. doi: 10.1089/ars.2010.3419.
50. Ranchoux B, Meloche J, Paulin R, Boucherat O, Provencher S, Bonnet S. DNA damage and pulmonary hypertension. *Intl J Mol Sci*. 2016;17:E990. doi: 10.3390/ijms17060990.
51. Meloche J, Pflieger A, Vaillancourt M, Paulin R, Potus F, Zervopoulos S, Graydon C, Courboulin A, Breuils-Bonnet S, Tremblay E, Couture C, Michelakis ED, Provencher S, Bonnet S. Role for DNA damage signaling in pulmonary arterial hypertension. *Circulation*. 2014;129:786–797. doi: 10.1161/CIRCULATIONAHA.113.006167.
52. Meloche J, Lampron MC, Nadeau V, Maltais M, Potus F, Lambert C, Tremblay E, Vitry G, Breuils-Bonnet S, Boucherat O, Charbonneau E, Provencher S, Paulin R, Bonnet S. Implication of inflammation and epigenetic readers in coronary artery remodeling in patients with pulmonary arterial hypertension. *Arterioscler Thromb Vasc Biol*. 2017;37:1513–1523. doi: 10.1161/ATVBAHA.117.309156.
53. Meloche J, Potus F, Vaillancourt M, Bourgeois A, Johnson I, Deschamps L, Chabot S, Ruffenach G, Henry S, Breuils-Bonnet S, Tremblay È, Nadeau V, Lambert C, Paradis R, Provencher S, Bonnet S. Bromodomain-containing protein 4: the epigenetic origin of pulmonary arterial hypertension. *Circ Res*. 2015;117:525–535. doi: 10.1161/CIRCRESAHA.115.307004.
54. Hansen T, Galougahi KK, Celermajer D, Rasko N, Tang O, Bubb KJ, Figtree G. Oxidative and nitrosative signalling in pulmonary arterial hypertension: implications for development of novel therapies. *Pharmacol Ther*. 2016;165:50–62. doi: 10.1016/j.pharmthera.2016.05.005.
55. Patel RS, Ghasemzadeh N, Eapen DJ, Sher S, Arshad S, Ko YA, Veledar E, Samady H, Zafari AM, Sperling L, Vaccarino V, Jones DP, Quyyumi AA. Novel biomarker of oxidative stress is associated with risk of death in patients with coronary artery disease. *Circulation*. 2016;133:361–369. doi: 10.1161/CIRCULATIONAHA.115.019790.
56. Griffith OW. Biologic and pharmacologic regulation of mammalian glutathione synthesis. *Free Radic Biol Med*. 1999;27:922–935.
57. Kieliszek M, Błażejak S. Selenium: significance, and outlook for supplementation. *Nutrition*. 2013;29:713–718. doi: 10.1016/j.nut.2012.11.012.
58. Sutendra G, Michelakis ED. Pulmonary arterial hypertension: challenges in translational research and a vision for change. *Sci Transl Med*. 2013;5:208sr205. doi: 10.1126/scitranslmed.3005428.
59. Paulin R, Dromparis P, Sutendra G, Gurtu V, Zervopoulos S, Bowers L, Haromy A, Webster L, Provencher S, Bonnet S, Michelakis ED. Sirtuin 3 deficiency is associated with inhibited mitochondrial function and pulmonary arterial hypertension in rodents and humans. *Cell Metabolism*. 2014;20:827–839. doi: 10.1016/j.cmet.2014.08.011.
60. Bonnet S, Archer SL, Allalunis-Turner J, Haromy A, Beaulieu C, Thompson R, Lee CT, Lopaschuk GD, Puttagunta L, Bonnet S, Harry G, Hashimoto K, Porter CJ, Andrade MA, Thebaud B, Michelakis ED. A mitochondria-K+ channel axis is suppressed in cancer and its normalization promotes apoptosis and inhibits cancer growth. *Cancer Cell*. 2007;11:37–51. doi: 10.1016/j.ccr.2006.10.020.
61. Youle RJ, van der Bliek AM. Mitochondrial fission, fusion, and stress. *Science*. 2012;337:1062–1065. doi: 10.1126/science.1219855.
62. Wolin MS. Novel role for the regulation of mitochondrial fission by hypoxia inducible factor-1α in the control of smooth muscle remodeling and progression of pulmonary hypertension. *Circ Res*. 2012;110:1395–1397. doi: 10.1161/CIRCRESAHA.112.270801.
63. Ryan JJ, Marsboom G, Fang YH, Toth PT, Morrow E, Luo N, Piao L, Hong Z, Ericson K, Zhang HJ, Han M, Haney CR, Chen CT, Sharp WW, Archer SL. PGC1α-mediated mitofusin-2 deficiency in female rats and humans with pulmonary arterial hypertension. *Am J Respir Crit Care Med*. 2013;187:865–878. doi: 10.1164/rccm.201209-1687OC.
64. Ryan J, Dasgupta A, Huston J, Chen KH, Archer SL. Mitochondrial dynamics in pulmonary arterial hypertension. *J Mol Med (Berl)*. 2015;93:229–242. doi: 10.1007/s00109-015-1263-5.
65. Diebold I, Hennigs JK, Miyagawa K, Li CG, Nickel NP, Kaschwich M, Cao A, Wang L, Reddy S, Chen PI, Nakahira K, Alcazar MA, Hopper RK, Ji L, Feldman BJ, Rabinovitch M. BMPR2 preserves mitochondrial function and DNA during reoxygenation to promote endothelial cell survival and reverse pulmonary hypertension. *Cell Metab*. 2015;21:596–608. doi: 10.1016/j.cmet.2015.03.010.
66. Chen PI, Cao A, Miyagawa K, Tojais NF, Hennigs JK, Li CG, Sweeney NM, Inglis AS, Wang L, Li D, Ye M, Feldman BJ, Rabinovitch M. Amphetamines promote mitochondrial dysfunction and DNA damage in pulmonary hypertension. *JCI Insight*. 2017;2:e90427. doi: 10.1172/jci.insight.90427.
67. Kalogris C, Garulli C, Pietrella L, Gambini V, Pucciarelli S, Lucci C, Tilio M, Zabaleta ME, Bartolacci C, Andreani C, Giangrossi M, Iezzi M, Belletti B, Marchini C, Amici A. Sanguinarine suppresses basal-like breast cancer growth through dihydrofolate reductase inhibition. *Biochem Pharmacol*. 2014;90:226–234. doi: 10.1016/j.bcp.2014.05.014.
68. Bellinger FP, Raman AV, Rueli RH, Bellinger MT, Dewing AS, Seale LA, Andres MA, Uyehara-Lock JH, White LR, Ross GW, Berry MJ. Changes in selenoprotein P in substantia nigra and putamen in Parkinson's disease. *J Parkinsons Dis*. 2012;2:115–126. doi: 10.3233/JPD-2012-11052.

69. Barrett CW, Reddy VK, Short SP, Motley AK, Lintel MK, Bradley AM, Freeman T, Vallance J, Ning W, Parang B, Poindexter SV, Fingleton B, Chen X, Washington MK, Wilson KT, Shroyer NF, Hill KE, Burk RF, Williams CS. Selenoprotein P influences colitis-induced tumorigenesis by mediating stemness and oxidative damage. *J Clin Invest*. 2015;125:2646–2660. doi: 10.1172/JCI76099.
70. Huang, Li T, Li X, Zhang L, Sun L, He X, Zhong X, Jia D, Song L, Semenza GL, Gao P, Zhang H. HIF-1-mediated suppression of acyl-CoA dehydrogenases and fatty acid oxidation is critical for cancer progression. *Cell Rep*. 2014;8:1930–1942. doi: 10.1016/j.celrep.2014.08.028.
71. Bonnet S, Michelakis ED, Porter CJ, Andrade-Navarro MA, Thebaud B, Bonnet S, Haromy A, Harry G, Moudgil R, McMurtry MS, Weir EK, Archer SL. An abnormal mitochondrial-hypoxia inducible factor-1α-Kv channel pathway disrupts oxygen sensing and triggers pulmonary arterial hypertension in fawn hooded rats: similarities to human pulmonary arterial hypertension. *Circulation*. 2006;113:2630–2641. doi: 10.1161/CIRCULATIONAHA.105.609008.
72. Brunet A, Bonni A, Zigmond MJ, Lin MZ, Juo P, Hu LS, Anderson MJ, Arden KC, Blenis J, Greenberg ME. Akt promotes cell survival by phosphorylating and inhibiting a Forkhead transcription factor. *Cell*. 1999;96:857–868.
73. Abid MR, Yano K, Guo S, Patel VI, Shrikhande G, Spokes KC, Ferran C, Aird WC. Forkhead transcription factors inhibit vascular smooth muscle cell proliferation and neointimal hyperplasia. *J Biol Chem*. 2005;280:29864–29873. doi: 10.1074/jbc.M502149200.
74. Gopinath SD, Webb AE, Brunet A, Rando TA. FOXO3 promotes quiescence in adult muscle stem cells during the process of self-renewal. *Stem Cell Reports*. 2014;2:414–426. doi: 10.1016/j.stemcr.2014.02.002.
75. Saito Y, Sato N, Hirashima M, Takebe G, Nagasawa S, Takahashi K. Domain structure of bi-functional selenoprotein P. *Biochem J*. 2004;381(pt 3):841–846. doi: 10.1042/BJ20040328.
76. Hoe HS, Harris DC, Rebeck GW. Multiple pathways of apolipoprotein E signaling in primary neurons. *J Neurochem*. 2005;93:145–155. doi: 10.1111/j.1471-4159.2004.03007.x.
77. Fessel JP, West JD. Redox biology in pulmonary arterial hypertension (2013 Grover Conference Series). *Pulm Circ*. 2015;5:599–609. doi: 10.1086/683814.
78. Archer SL, Marsboom G, Kim GH, Zhang HJ, Toth PT, Svensson EC, Dyck JR, Gomberg-Maitland M, Thébaud B, Husain AN, Cipriani N, Rehman J. Epigenetic attenuation of mitochondrial superoxide dismutase 2 in pulmonary arterial hypertension: a basis for excessive cell proliferation and a new therapeutic target. *Circulation*. 2010;121:2661–2671. doi: 10.1161/CIRCULATIONAHA.109.916098.
79. Sturrock A, Cahill B, Norman K, Huecksteadt TP, Hill K, Sanders K, Karwande SV, Stringham JC, Bull DA, Gleich M, Kennedy TP, Hoidal JR. Transforming growth factor-beta1 induces Nox4 NAD(P)H oxidase and reactive oxygen species-dependent proliferation in human pulmonary artery smooth muscle cells. *Am J Physiol Lung Cell Mol Physiol*. 2006;290:L661–L673. doi: 10.1152/ajplung.00269.2005.
80. Guzy RD, Hoyos B, Robin E, Chen H, Liu L, Mansfield KD, Simon MC, Hammerling U, Schumacker PT. Mitochondrial complex III is required for hypoxia-induced ROS production and cellular oxygen sensing. *Cell Metab*. 2005;1:401–408. doi: 10.1016/j.cmet.2005.05.001.
81. Klatt P, Lamas S. Regulation of protein function by S-glutathiolation in response to oxidative and nitrosative stress. *Eur J Biochem*. 2000;267:4928–4944.
82. Watanabe Y, Murdoch CE, Sano S, Ido Y, Bachschmid MM, Cohen RA, Matsui R. Glutathione adducts induced by ischemia and deletion of glutaredoxin-1 stabilize HIF-1α and improve limb revascularization. *Proc Natl Acad Sci U S A*. 2016;113:6011–6016. doi: 10.1073/pnas.1524198113.
83. Sutendra G, Bonnet S, Rochefort G, Haromy A, Folmes KD, Lopaschuk GD, Dyck JR, Michelakis ED. Fatty acid oxidation and malonyl-CoA decarboxylase in the vascular remodeling of pulmonary hypertension. *Sci Transl Med*. 2010;2:44ra58. doi: 10.1126/scitranslmed.3001327.
84. Weir EK, López-Barneo J, Buckler KJ, Archer SL. Acute oxygen-sensing mechanisms. *N Engl J Med*. 2005;353:2042–2055. doi: 10.1056/NEJMra050002.
85. Peacock AJ, Murphy NF, McMurray JJ, Caballero L, Stewart S. An epidemiological study of pulmonary arterial hypertension. *Eur Respir J*. 2007;30:104–109. doi: 10.1183/09031936.00092306.
86. Hoeper MM, McLaughlin VV, Dalaan AM, Satoh T, Galiè N. Treatment of pulmonary hypertension. *Lancet Respir Med*. 2016;4:323–336. doi: 10.1016/S2213-2600(15)00542-1.
87. Takayama H, Misu H, Iwama H, Chikamoto K, Saito Y, Murao K, Teraguchi A, Lan F, Kikuchi A, Saito R, Tajima N, Shirasaki T, Matsugo S, Miyamoto K, Kaneko S, Takamura T. Metformin suppresses expression of the selenoprotein P gene via an AMP-activated kinase (AMPK)/FoxO3a pathway in H4IIEC3 hepatocytes. *J Biol Chem*. 2014;289:335–345. doi: 10.1074/jbc.M113.479386.